

RARE GENETIC CAUSES OF MICROCEPHALY AND MEGALENCEPHALY

Ph.D. Thesis

Melinda Zombor, M.D.

Department of Paediatrics, Faculty of Medicine, University of Szeged

Doctoral School of Clinical Medicine
Clinical and Experimental Neurosciences

Supervisor: László Sztriha, M.D., Ph.D., D.Sc.

Szeged

2020

THIS THESIS IS BASED ON THE FOLLOWING PUBLICATIONS

1. **Zombor M**, Kalmár T, Nagy N, Berényi M, Telcs B, Maróti Z, Brandau O, Sztriha L. A novel *WDR62* missense mutation in microcephaly with abnormal cortical architecture and review of the literature. *J Appl Genet* 2019;**60**:151-162. **(Impact factor: 1.725)**.
2. **Zombor M**, Kalmár T, Maróti Z, Zimmermann A, Máté A, Bereczki Cs, Sztriha L. Co-occurrence of mutations in *FOXP1* and *PTCH1* in a girl with extreme megalencephaly, callosal dysgenesis and profound intellectual disability. *J Hum Genet* 2018;**63**:1189-1193. **(IF:3.545)**
3. Alcantara D, Timms AE, Gripp K, Baker L, Park K, Collins S, Cheng C, Stewart F, Mehta SG, Saggari A, Sztriha L, **Zombor M**, Caluseriu O, Mesterman R, Van Allen MI, Jacquinet A, Ygberg S, Bernstein JA, Wenger AM, Guturu H, Bejerano G, Gomez-Ospina N, Lehman A, Alfei E, Pantaleoni C, Conti V, Guerrini R, Moog U, Graham JM, Hevner R, Dobyns WB, O'Driscoll M, Mirzaa GM. Mutations of *AKT3* are associated with a wide spectrum of developmental disorders including extreme megalencephaly. *Brain* 2017;**40**:2610-2622. **(IF:10.840)**.

TABLE OF CONTENTS	Page
SUMMARY	4
ÖSSZEFOGLALÁS	6
INTRODUCTION	8
OBJECTIVES	10
METHODS	10
PATIENTS AND RESULTS	12
DISCUSSION	16
CONCLUSIONS	32
ACKNOWLEDGEMENTS	32
TABLE	33
FIGURES	34
REFERENCES	47

SUMMARY

Microcephaly has been defined as an occipitofrontal head circumference of equal to or less than 2-3 standard deviations below the mean related for age and gender. It may develop prenatally (congenital microcephaly) or postnatally and may have genetic or non-genetic causes. Although a wide spectrum of genetic defects can result in microcephaly, traditionally a group of microcephalies has been distinguished as autosomal recessive primary microcephaly (MicroCephal Primary Hereditary, MCPH).

Both **megalencephaly** and **macrocephaly** have been defined as conditions with head circumference that exceeds the mean by 2 or more standard deviations (SD) for age and gender. *Megalencephaly* refers to an enlarged brain due to increased growth of cerebral structures during brain development, while in *macrocephaly* the enlarged head is the result of hydrocephalus, subdural fluid collections or intracranial masses. Megalencephaly can be idiopathic, or can be associated with metabolic disorders, or genetic syndromes.

Objectives

The aims of this study were to characterize the phenotypic and genotypic features of three patients with autosomal recessive primary *microcephaly* and two children with *megalencephaly*.

Methods

Thorough assessment of the patients has been carried out including physical and neurological examination and developmental testing. Chromosomal analysis and array comparative genome hybridization (aCGH) were performed, followed by next generation sequencing. Whole exome sequencing (WES) was performed for three patients with autosomal recessive primary microcephaly (*ASPM* and *WDR62* genes, CentoXome® at Centogene AG, Rostock, Germany). The Illumina Trusight One Exome Sequencing Panel (Illumina Inc., San Diego, California, USA) was used for the analysis of mutations in two genes (*FOXP1* and *PTCH1*) in a girl with megalencephaly (Department of Paediatrics, University of Szeged). Multiplex targeted sequencing was applied using single molecule molecular inversion probes in the patient with megalencephaly and *AKT3* mutation (in collaboration with scientists in the USA). The mutations were confirmed by Sanger sequencing.

Patients and Results

Patient 1./ A novel homozygous nonsense variant in the *ASPM* gene [c.7323T>A, p.(Tyr2441Ter)] in exon 18 in a boy was associated with congenital microcephaly, severe developmental delay and MRI features of cortical dysplasia and polymicrogyria.

Patients 2 and 3./ A boy and a girl had the same novel homozygous missense variant [c.668T>C, p.(Phe223Ser)] in exon 6 in the *WDR62* gene. They had hemispherical asymmetry and diffuse pachygyria on the MRI in addition to microcephaly and severe developmental delay, Haplotype analysis suggested close relationship between the families of these patients.

Patient 4./ A girl with extreme megalencephaly and profound intellectual disability had *de novo* heterozygous variants in exon 18 of the *FOXP1* [c.1573C>T, p.(Arg525Ter)] gene and exon 17 of the *PTCHI* [c.2834delGinsAGATGTTGTGGACCC, p.(Arg945GlnfsTer22)] gene. The *PTCHI* mutation was novel.

Patient 5./ Megalencephaly, diffuse polymicrogyria and delayed development were the characteristic features of a boy with an activating *de novo* germline heterozygous missense variant [c.1393C>T; p.(Arg465Trp)] in exon 13 of the *AKT3* gene, which encodes a member of the PI3K (phosphatidylinositol-3-kinase)–AKT (*AK mouse* + *Transforming* or *Thymoma*)-mTOR) pathway.

Conclusions

Rare autosomal recessive primary microcephaly (MCPH) due to mutations in *ASPM* and *WDR62* might be the result of abnormal function of the centrosomes, which organize the separation of chromosome copies during cell division. Megalencephaly in association with pathogenic mutations in two genes (*FOXP1* and *PTCHI*) in the same individual is exceptionally rare and the severe phenotype might have been the result of the combined effect of this genetic constellation. Activating mutation in a gene (*AKT3*) encoding a member of the PI3K-AKT-mTOR pathway in association with megalencephaly is also a rare condition. It is justified therefore, to devote this study to the thorough work up of these patients; it is in line with the international endeavour to identify the genetic causes of rare diseases by applying new technologies, particularly array methods and next generation sequencing.

ÖSSZEFOGLALÁS

Microcephaliában a fejkörfogat kisebb, mint az életkorra és nemre jellemző 2 standard deviáció (SD). Microcephalia kialakulhat prenatalisan (congenitalis microcephalia), vagy postnatalisan, mindkét esetben az etiológia lehet genetikai rendellenesség, vagy környezeti ártalom. Bár rendkívül sokféle genetikai defektus okozhat microcephaliát, a szakirodalom megkülönbözteti az autoszomális recesszív primer microcephaliák (MicroCephal Primary Hereditary, MCPH) csoportját.

Megalencephalia és **macrocephalia** esetén a fejkörfogat meghaladja az életkorra és nemre vonatkoztatott 2 standard deviációt (SD). *Megalencephalia* az agyi struktúrák fokozott növekedésére utal, míg *macrocephaliáról* beszélünk hydrocephalus, subduralis folyadékgyülem, vagy egyéb intracranialis térszűkítő folyamat esetén. A megalencephalia lehet idiopathiás, veleszületett anyagcsere betegség következménye, vagy társulhat genetikai szindrómákhoz.

Célkitűzések

Átnézve a SZTE Gyermekklinika B Részlegének Neurológiai Szakrendelésén vizsgált betegek adatait, 3 beteget találtunk, akik ritka autoszomális recesszív primer *microcephaliában* szenvedtek, 2 beteget pedig *megalencephaliával* azonosítottunk. Célul tűztük ki az 5 beteg fenotípusának és genotípusának az elemzését.

Módszerek

Fizikális és neurológiai vizsgálat történt, továbbá a fejlődést is értékeltük. Kromoszóma vizsgálat és array összehasonlító genomiális hibridizáció után új generációs szekvenálás következett. A három, *microcephaliában* szenvedő beteg mutációját az *ASPM* és *WDR62* génben teljes exom szekvenálás (WES) derítette ki (CentoXome®) a Centogene Laboratóriumban, Németországban. Az Illumina Trusight One Exome Sequencing Panel (Illumina Inc., San Diego, California, USA) alkalmazásával sikerült megtalálni a mutációt két génben (*FOXPI* és *PTCH1*) az SZTE Gyermekgyógyászati Klinikán egy *megalencephaliában* szenvedő leányban. Egy fiúban pedig többszörös célzott szekvenálással (multiplex targeted sequencing using single molecular inversion probes) derült ki mutáció az *AKT3* génben, mint a *megalencephalia* oka az Amerikai Egyesült Államokban. Sanger szekvenálással megerősítettük a mutációkat.

Betegek és eredmények

1. beteg. Az *ASPM* gén egy új, eddig nem közölt homozigóta mutációja [exon 18: c.7323T>A, p.(Tyr2441Ter)] okozott súlyos congenitalis *microcephaliát*, corticalis displasiát és polymicrogyriát egy fiúban, akinek a fejlődése súlyosan késlekedett.

2-3. *beteg*. A *WDR62* gén új és azonos homozigóta mutációja [exon 6: c.668T>C, p.(Phe223Ser)] derült ki egy fiúban és egy leányban, akik súlyos congenitalis microcephaliában szenvedtek. Fejlődésük súlyosan késlekedett, az MRI pedig az agyi féltekék aszimmetriáját és pachygyriát mutatott. A haplotípus analízis rokonságot valószínűsített a betegek családjai között.

4. *beteg*. Egy leányban *de novo* heterozigóta patogén mutációt találtunk a *FOXPI* [exon 18: c.1573C>T, p.(Arg525Ter)] és a *PTCHI* [exon 17: c.2834delGinsAGATGTTGTGGACCC, p.(Arg945GlnfsTer22)] génben. A *PTCHI* mutáció új, még nem közölt variáns.

5. *beteg*. Egy fiúban, akinek késlekedett a fejlődése, diffúz polymicrogyria társult a megalencephaliához. A molekuláris vizsgálat során *de novo* germline heterozigóta missense mutáció [exon 13: c.1393C>T; p.(Arg465Trp)] igazolódott az *AKT3* génben.

Következtetések

Az *ASPM* és *WDR62* gének által kódolt fehérjék szükségesek a centrosomák normális funkciójához. Ezek az organellumok fontos szerepet játszanak a sejtosztódásban, és kóros működésük autoszomális recesszív primer microcephaliát eredményez. Megalencephalia két gén (*FOXPI* és *PTCHI*) patogén mutációjának következtében egy betegben rendkívül ritka. A kifejezett megalencephalia és a súlyos értelmi fogyatékoság a két mutáció *együttes* hatásának lehetett a következménye. Megalencephalia a PI3K-AKT-mTOR jelátviteli rendszer egyik elemét kódoló gén (*AKT3*) aktiváló mutációja következtében szintén ritka. Betegeink tanulmányozása és eredményeink disszertációba foglalása összhangban van azokkal a nemzetközi törekvésekkel, amelyek az új genetikai technológiák alkalmazásával kutatják a ritka betegségek okait.

INTRODUCTION

Microcephaly has been defined as an occipitofrontal head circumference of equal to or less than 2-3 standard deviations (SD) below the mean related for age and gender (Zaqout et al., 2017, Jayaraman et al., 2018). Microcephaly may develop prenatally (congenital microcephaly) or postnatally and may have genetic or non-genetic causes. Any condition that affects important processes of brain growth, including progenitor cell proliferation, cell differentiation, and cell death, can lead to microcephaly (von der Hagen et al., 2014, Zaqout et al., 2017). Anomalies causing microcephaly may exclusively affect cerebral development (non-syndromic microcephaly) or may be associated with dysmorphic features and extracerebral malformations (syndromic microcephaly) (von der Hagen et al., 2014). The spectrum of phenotypes and associated disorders of “microcephaly” is wide with 1429 entries recorded to September 2019 in The Online Mendelian Inheritance in Man (OMIM) database.

Although a wide spectrum of genetic defects can result in microcephaly, traditionally a group of microcephalies is distinguished as autosomal recessive primary microcephaly (MicroCephalo Primary Hereditary, MCPH) (Zaqout et al., 2017). At least 18 genetic loci (MCPH1-18 until September 2019) have been implicated in MCPH, all of which have now been connected to single genes: *MCPH1*, *WDR62*, *CDK5RAP2*, *CASC5*, *ASPM*, *CENPJ*, *STIL*, *CEP135*, *CEP152*, *ZNF335*, *PHC1*, *CDK6*, *CENPE*, *SASS6*, *MFSD2A*, *ANKLE2*, *CIT*, *WDFY3* (Jayaraman et al., 2018). Many of the proteins encoded by these genes interact with the centrosomes, which organizes the separation of chromosome copies during cell division. The architecture of the small brain with simplified gyral pattern was not grossly affected in patients described initially, subsequent studies, however, revealed a wide spectrum of cortical malformations in association with MCPH of different aetiologies, particularly *WDR62* mutations (Jayaraman et al., 2018, Shohayeb et al., 2018).

We report on three patients who had autosomal recessive primary microcephaly in association with abnormal cortical architecture: a boy with a novel nonsense mutation in the *ASPM* gene (OMIM 605481; abnormal spindle-like, microcephaly-associated protein, MicroCephalo Primary Hereditary 5, chromosome 1q31.3) and two other patients, a boy and a girl with the same novel missense mutations in *WDR62* (OMIM 613583; WD repeat containing protein 62, MicroCephalo Primary Hereditary 2, chromosome 19q13.12).

Megalencephaly and **macrocephaly** have been defined as conditions with head circumference above the age-related mean by 2 or more standard deviations.

Megalencephaly defines an increased growth of cerebral structures because of either increased size or number of neurons and glial cells. In contrast, in *macrocephaly*, the increased head circumference is linked to hydrocephalus, subdural fluid collections, or intracranial masses (Mirzaa and Poduri, 2014, Pavone et al., 2017).

Megalencephaly can be *idiopathic/benign* or it can be associated with *metabolic disorders*, or *genetic syndromes*.

Idiopathic/benign megalencephaly refers to children who have an abnormally large head with no neurological impairment. An increased head circumference is often reported in one or both the parents as well.

In *metabolic megalencephaly*, the clinical course is usually progressive with a more or less rapid neurological impairment. Defects in the organic acid metabolism, like glutaric aciduria type 1, or L-2-hydroxyglutaric aciduria are associated with megalencephaly. Several forms of leukoencephalopathies, such as Canavan disease, Alexander disease, megalencephalic leukoencephalopathy with subcortical cysts can cause megalencephaly. Accumulation of metabolic substrates is also accompanied with megalencephaly in lysosomal storage disorders, such as Tay-Sachs disease, Sandhoff disease, or mucopolysaccharidoses (Mirzaa and Poduri, 2014, Pavone et al., 2017).

Megalencephaly is a phenotypic feature of Sotos, Weaver, Simpson-Golabi-Behmal, *PTEN* hamartoma tumour and Gorlin syndromes among others. Recently, megalencephaly as a presenting sign has been reported in megalencephaly-polymicrogyria-polydactyly-hydrocephalus (MPPH) syndrome. Mostly *de novo* germline or somatic mutations in *PIK3R2* (chromosome 19p13.11) and *AKT3* (chromosome 1q43-q44) have been found in this disorder. These genes encode members of the PI3K-AKT-mTOR pathway (Mirzaa and Poduri, 2014, Pavone et al., 2017).

The phenotypic features and molecular genetic findings of two patients with megalencephaly are presented in this study. A girl with extreme megalencephaly and profound intellectual disability had *de novo* mutations in two genes, such as *FOXP1* (forkhead box protein P1; OMIM 605515, chromosome 3p13) and *PTCH1* (*patched homolog 1*, OMIM 601309, chromosome 9q22.3). Megalencephaly, diffuse polymicrogyria and delayed development were the characteristic features of a boy with a germline *de novo* mutation in *AKT3* (*AK mouse + Transforming or Thymoma*, OMIM 611223, chromosome 1q43-q44).

Autosomal recessive primary microcephaly due to *ASPM* or *WDR62* mutations are rare conditions. Megalencephaly in association with pathogenic mutations in two genes

(*FOXP1* and *PTCHI*) in the same individual and activating mutation in a member of the PI3K-AKT-mTOR pathway is also very rare. It is justified therefore to devote this study to the thorough work up of these patients. It is in line with the international endeavour to identify the genetic causes of rare diseases by applying new technologies, particularly array methods and next generation sequencing.

OBJECTIVES

The aims of this study were

- 1./ to ascertain patients with rare forms of *autosomal recessive primary microcephaly* and *megalencephaly*
- 2./ to assess these patients, including physical and neurological examination and developmental testing
- 3./ to evaluate the brain MR images
- 4./ to identify the molecular genetic causes of these conditions

METHODS

Patients with autosomal recessive primary microcephaly (3 children) and megalencephaly (2 children) were enrolled out of the patient population referred to the Paediatric Neurology Service (outpatient and inpatient), Department of Paediatrics, Division B, University of Szeged, Hungary between 1 January 2006 and 31 December 2017.

Standard assessment included clinical history of the antenatal, perinatal, neonatal, and postnatal period. Physical and neurological examinations were carried out. Special attention has been paid to the presence of dysmorphic features and malformations. A standardized vocabulary of phenotypic abnormalities, provided by the Human Phenotype Ontology has been applied. Hearing was always tested and neuro-ophthalmologic consultation was also an integral part of the examinations. The developmental milestones, cognitive and behavioural phenotypes were also assessed. Screening for inborn errors of metabolism and intrauterine infections were carried out by conventional methods. Brain MRI was performed in axial, coronal and sagittal planes.

Routine chromosomal analysis occurred by G-banding. Genomic DNA was isolated from the peripheral blood in all patients and also from saliva in Patient 5. Array comparative genomic hybridization was performed using the Affymetrix 750K array.

In **Patients 1-3** whole exome sequencing (WES trio) was performed with CentoXome[®] at Centogene AG (Rostock, Germany). Genomic capture was carried out with Illumina's Nextera Rapid Capture Exome Kit. Massively parallel sequencing was done using NextSeq500 Sequencer (Illumina) in combination with the NextSeq™ 500 High Output Kit (2x150bp). Raw sequence data analysis, including base calling, demultiplexing, alignment to the hg19 human reference genome (Genome Reference Consortium GRCh37), and variant calling, were performed using an in house bioinformatics pipeline. For variant filtration, all disease-causing variants reported in Human Gene Mutation Database (HGMD[®]), ClinVar or in CentoMD[®] as well as all variants with minor allele frequency (MAF) of less than 1% in Exome Aggregation Consortium (ExAc) database were considered. Variants that possibly impair the protein sequence, i.e. disruption of conserved splice sites, missense, nonsense, read-throughs, or small insertions/deletions, were prioritized. All relevant inheritance patterns were considered.

In **Patient 4** the Illumina Trusight One Exome Sequencing Panel (Illumina Inc., San Diego, CA, USA), covering the coding region of 4,813 clinically relevant genes, was applied using Illumina MiSeq (Illumina Inc., San Diego, California, USA). Variants were filtered based on severity and frequency against public variant databases including single-nucleotide polymorphism database (dbSNP), ClinVar, ExAC, Exome Variant Server (EVS) and in-house clinical exome database of 140 unrelated Hungarian persons. All relevant inheritance patterns were considered.

In **Patient 5** multiplex targeted sequencing was applied using single molecule molecular inversion probes (smMIP, Hiatt et al., 2013, Alcantara et al., 2017).

All candidate pathogenic variants were confirmed by conventional PCR amplification and Sanger sequencing. Segregation of these changes with the disease was assessed for all available family members.

Haplotype analysis of the families

Since the families of **Patients 2-3** with the same *WDR62* mutation were unaware of any relation between them, we performed a haplotype analysis to investigate their potential genetic relation. Plink (version v1.90b4.9) was used to convert variants in the region of interest to Pedigree (PED) and MAP files from the joint Variant Call Format (VCF) file (Chang et al., 2015). Haplotype analysis was performed by Merlin (version 1.1.2.) software with the "--best" option using the PED, Data (DAT), and MAP files prepared manually from the plink output files (Abecasis et al., 2002). HaploPainter

(version 1.043) was used to visualize the haplotypes in the families (Thiele and Nürnberg, 2005).

An *informed consent* to participate in this study was requested from the parents. This study was approved by the *Human Investigation Review Board, University of Szeged, Albert Szent-Györgyi Clinical Center (3797/2016)*.

PATIENTS AND RESULTS (Table 1)

MICROCEPHALY (PATIENTS 1-3)

Patient 1 - *ASPM* mutation

This boy was born from the first pregnancy to unrelated healthy parents at 36th gestational week. Apgar scores were 9 and 10 at 1 and 5 minutes, respectively. His birth weight was 2350 g (-0.9 SD), length 47 cm (-0.1 SD). Microcephaly was noted at birth with head circumference of ~30 cm (-1.8 SD). The pregnancy was complicated by threatened abortion, however there were no report of infection, alcohol use or substance abuse. The microcephaly progressed with head circumference of 39 cm (-5.1 SD) at 10 months, 40,5 cm (-5.2 SD) at 18 months, and 43.5 cm (-5.7 SD) at 5,5 years of age. His weight was 18 kg (-0.4 SD) and height 110 cm (-0.7 SD) at this age. Sloping forehead and disproportionately large face and ears as compared to the skull were observed. Motor and intellectual development was severely impaired with inability to sit and stand unsupported or speak at the age of 5 years. He followed objects and responded to loud sounds. Typical signs of spastic tetraplegia (spastic quadriplegia) were observed. Tonic-clonic seizures appeared at the age of 18 months and the interictal EEG showed bilateral symmetric and asymmetric spike and wave discharges. The seizures were well controlled with valproate.

Brain MRI at age of 7 months showed an abnormal cortical pattern with features of cortical dysplasia and polymicrogyria. The grey-white matter junction appeared indistinct at some areas. The Virchow-Robin spaces and lateral ventricles were dilated (Fig. 1. A, B, C).

The WES trio (Centogene AG) identified a novel homozygous pathogenic variant, c.7323T>A, p.(Tyr2441Ter) in exon 18 of the *ASPM* gene in the patient (Fig. 2). This variant creates a premature stop codon and it is consistent with the diagnosis of autosomal recessive primary microcephaly type 5. The detected variant was also found in heterozygous state in the patient's parents. To date this variant has not been described in

the Exome Aggregation Consortium, Exome Sequencing Project or the 1000 Genome Browser.

Patient 2 – *WDR62* mutation

This boy was born at term from the third pregnancy with Cesarean section to healthy consanguineous parents of Romani ethnicity (Fig. 3 A). Apgar scores were 8 and 8 at 1 and 5 minutes, respectively. Severe microcephaly was noted at birth with head circumference of 30 cm (-3.5 SD). The birthweight was 2900 g (-1.0 SD) and length 50 cm (0.1 SD). The pregnancy was unremarkable, with no report of infection, alcohol use or substance abuse. The parents have a healthy son and a healthy daughter. Microcephaly progressed, with head circumference of 40 cm (-6.0 SD) at 2 years and 41.5 cm (-6.0 SD) at 4 years of age. The patient also had failure to thrive with a height of 89 cm (-3.4 SD) and a weight of 12 kg (-2.4 SD) at 4 years of age. Sloping forehead and disproportionately large face and ears as compared to the skull were observed. He followed objects and responded to loud sounds. His motor and intellectual development was severely impaired with inability to sit and stand unsupported, or reach out for objects at the age of 5 years. He had no words, but showed emotions. Global hypotonia was present with preserved deep tendon reflexes. Infantile spasms began at 4 months of age and were well controlled with vigabatrin, which was tapered off and discontinued by 3 years of age. One year later complex partial seizures appeared and the EEG showed interictal short paroxysms of bilateral spike and wave discharges. Valproate treatment was initiated and proved to be successful.

MRI at age of 5 months showed hemispherical asymmetry (R>L) and abnormal cortical pattern. Diffuse pachygyria was observed with a few broad gyri, thick grey matter and shallow sulci (Fig. 4 A, B).

Patient 3 – *WDR62* mutation

This girl was born at term from the first pregnancy with Cesarean section because of fetal bradycardia to healthy parents of Romani ethnicity. They denied consanguinity (Fig. 3 B). Apgar scores were 7, 9 and 10 at 1, 5 and 10 minutes, respectively. The pregnancy was complicated with urinary tract infection. Severe microcephaly was noted at birth with head circumference of 28 cm (-5.0 SD). Her birthweight was 2490 g (-0.4 SD) and length 46 cm (-1.7 SD). There was no evidence of intrauterine infection, alcohol use or substance abuse. Microcephaly progressed, with head circumference of 39 cm (-5.9 SD) at 2 years and 40 cm (-6.6 SD) at 4 years of age. The patient also had signs of failure to thrive with height of 88 cm (-3.4 SD) and weight of 12,4 kg (-2.0 SD) at 4 years of age.

On examination at the age of 14 months she had severe convergent squint, but followed objects and responded to loud sounds. Her motor and cognitive development was severely lagged behind with inability to sit, stand or reach out for objects. There was a moderate decrease in the muscle tone with slight left sided weakness and preserved deep tendon reflexes. No further development was observed until the last follow up at 5 years of age. Complex partial seizures started after 3 years of age and the interictal EEG showed bilateral spike and wave discharges. The epilepsy was well controlled with valproate treatment.

MRI at the age of 4 years showed hemispherical asymmetry (L>R) and abnormal cortical pattern similar to Patient 2 (Fig. 4, C, D).

WES trio (Centogene AG) identified the same novel homozygous missense variant, c.668T>C, p.(Phe223Ser) in exon 6 in the *WDR62* gene in Patients 2 and 3. The detected variant was also found in heterozygous state in the patients' parents and the brother of Patient 2 (Fig. 3. A, B, C). To date this variant has not been described in the Exome Aggregation Consortium, Exome Sequencing Project or the 1000 Genome Browser. It is located in a highly conserved nucleotide (phyloP: 4.48) with large physicochemical differences between the exchanged amino acids Phenylalanine and Serine (Alamut v.2.7.1). Prediction programs Polyphen2, SIFT and MutationTaster predicted pathogenicity of the variant which affects the WD40 repeat region of the protein (Fig. 3. D), whereas Align-GVGD predicted toleration.

The family members of Patients 2 and 3 were unaware of any relatedness. Haplotype analysis showed that both families carry exactly the same haplotype for the entire *WDR62* gene (around 55 kilobases) as shown in Fig. 5. Our results, therefore, suggest that the two families are closely related genetically.

MEGALENCEPHALY (PATIENTS 4-5)

Patient 4 – Coexistence of *FOXP1* and *PTCH1* mutation

The proband, a girl was born as the second child to healthy, non-consanguineous parents at 36 weeks of gestation via vaginal delivery with birth weight of 2,870 g (0.4 SD), length of 50 cm (0.8 SD) and head circumference of 37 cm (1.8 SD). Apgar scores were 8, 9 and 10 at 1, 5 and 10 minutes, respectively. There was no evidence of intrauterine infection or inborn error of metabolism.

Several dysmorphic features were noticed (Fig. 6 A, B, D). Progressive growth of her head circumference was noted; it was 58 cm (6.1 SD) at the age of 4 years, and 61 cm

(7.1 SD) at the age of 8 years (Fig. 6 C). Her height was 129 cm (0.2 SD) and weight 33 kg (1.3 SD) at 8 years of age. On examination, her hearing proved to be normal. She required glasses because of severe myopia. Generalized hypotonia, unstable gait and preserved deep tendon reflexes were observed. Her motor and cognitive development was severely delayed with inability to speak or follow commands at the age of 8 years. Brunet-Lézine test at the age of 2.5 years showed a developmental quotient of 40. She had temporary outbursts of aggressive behaviour.

Brain MRI, performed at 3 months, 3 and 4 years of age revealed partial agenesis of the corpus callosum and widely separated leaves of the septum pellucidum (Fig, 6 E, F). Brain CT was not performed. Abdominal and cardiac ultrasound, chest X-ray and dental radiography were normal.

Chromosomal analysis showed a normal 46,XX karyotype. Copy number changes were not found by Affymetrix 750K array. Clinical exome (Trusight One panel) sequencing revealed heterozygous variants in exon 18 of the *FOXP1* [c.1573C>T, p.(Arg525Ter)] and exon 17 of the *PTCH1* [c.2834delGinsAGATGTTGTGGACCC, p.(Arg945GlnfsTer22)] genes in the patient (Figs. 7, 8). The *FOXP1* variant has been reported earlier as a nonsense pathogen mutation (rs112795301, RCV000005214), while the *PTCH1* variant has not been found in either dbSNP, ClinVar, ExAC, or EVS databases or a cohort of 140 unrelated Hungarian controls. Sanger sequencing confirmed both variants as *de novo* mutations in the patient. They were not present either in the parents or in the patient's healthy brother (Figs. 7, 8).

Patient 5 - *AKT3* mutation

The patient, a boy was born by Cesarean section from the second uneventful pregnancy at 36th gestational weeks to unrelated healthy Caucasian parents. His birthweight was 3280g (1.3 SD), length 50 cm (1.2 SD) and head circumference 37.5 cm (3.3 SD). There was no history of alcohol use or substance abuse and there was no evidence of intrauterine infection or inborn error of metabolism. The infant did not have hypoglycaemia. He had a healthy brother.

His head circumference was 51 cm (5.1 SD) at 7 months of corrected age, 53 cm (4.5 SD) at 15 months and 55 cm (4.1 SD) at 28 months of age. His weight was 11.5 kg (-1.3 SD) and height 82 cm (-2.2 SD) at this age. Dysmorphic features, such as bossing forehead, wide nasal bridge, short nose and bilateral partial cutaneous syndactyly of III-IV toes were observed. At the age of 3 years, his vision and hearing were normal, however, he had severe chewing impairment and did not speak. Connective tissue laxity,

muscular hypoplasia, generalized hypotonia and weakness were noticed. The deep tendon reflexes were preserved. He was able to stand and make a few steps. Recurrent tonic-clonic seizures with and without fever appeared after the age of 11 months. They were well controlled with levetiracetam and an EEG at the age of 2.5 years did not show epileptiform discharges.

MRI was performed at 7 months of age and it revealed polymicrogyria in the perisylvian, frontal, parietal and temporal areas on both sides (Fig. 9).

Chromosomal analysis showed a normal 46,XY karyotype. Targeted next generation sequencing (Alcantara et al., 2017) revealed a heterozygous missense variant [c.1393C>T, p.(Arg465Trp)] in exon 13 of the *AKT3* gene (Fig. 10 A,B). This pathogenic variant was present in 50% of reads in the DNA samples derived from both the blood and saliva, suggesting a constitutional mutation. The mutation was confirmed by Sanger sequencing. It was a *de novo* mutation, absent in the parental samples.

DISCUSSION

MICROCEPHALY

Proliferation of the neural progenitor cells

Brain size at birth is primarily dependent on the ability of neural progenitor cells (neuroepithelial cells, radial glia cells and short neural precursors with apical-basal polarity lining the ventricles of the foetal brain) to proliferate and self-renew. While symmetrical division of a neural progenitor cell results in the generation of two identical neural progenitor cells (thereby increasing the progenitor pool), asymmetrical division leads to the production of one progenitor cell (thereby maintaining the progenitor pool) and a committed precursor, which eventually undergoes migration and differentiates into neuron (Dehay and Kennedy, 2007, Fish et al., 2008, Uzquiano et al., 2018; Explanatory figure 1, 2).

The cell cycle of eukaryotic cells can be divided into four successive phases: M phase (mitosis), S phase (DNA synthesis) and two gap phases, G1 and G2. Centrosomes play an essential role in cell division, as they are responsible for the formation and maintenance of the microtubule-based spindle apparatus. The centrosome contains a pair of cylindrical centrioles in an orthogonal configuration. The centrioles are surrounded by pericentriolar matrix of proteins and centrosomal satellites. The satellites are granular structures implicated in the trafficking of material involved in centriole assembly. Centriole duplication occurs during each cell-cycle and both centrioles and centrosomes

undergo final maturation in the G2 and M phases (Prosser and Pelletier, 2017, Nigg and Holland, 2018, Explanatory figure 3/A). Centrosome duplication in dividing neuroprogenitors generates a pair of centrosomes with differently aged mother centrioles. During peak phases of neurogenesis the centrosome retaining the old mother centriole stays in the ventricular zone and is preferentially inherited by neuroprogenitors, whereas the centrosome containing the new mother centriole mostly leaves the ventricular zone and is largely associated with differentiating cells (Wang et al., 2009, Explanatory figure 3/C).

Centrosomal duplication results in the generation of a bipolar mitotic spindle (Explanatory figure 3/B). The chromosomes attach to bundles of microtubules via kinetochores, which are multiprotein complexes that assemble on the centromere of each sister chromatid (Prosser and Pelletier, 2017). The mitotic processes are dependent also upon the highly conserved Chromosomal Passenger Complex, consisting of Aurora B kinase, INner CENtromere Protein (INCENP), Survivin and Borealin. Aurora B is the enzymatically active member of the complex. INCENP functions as a scaffolding protein, while Survivin and Borealin are targeting subunits. This complex targets to different locations at differing times during mitosis, where it regulates key mitotic events, such as correction of kinetochore-microtubule attachment errors, activation of the spindle assembly checkpoint, and construction and regulation of the contractile apparatus that drives cytokinesis (Carmena et al., 2012).

***ASPM* and *WDR62* encode centrosomal proteins functioning in the division of neural progenitor cells (Explanatory figure 4)**

ASPM (OMIM 605481; abnormal spindle-like, microcephaly-associated protein) mutations cause MCPH5 (MicroCephalY Primary Hereditary 5), while *WDR62* (OMIM 613583; WD repeat containing protein 62) mutations are responsible for MCPH2. These are the most common causes of autosomal recessive primary microcephaly (Zaqout et al., 2017). *ASPM* maps at 1q31.3 locus. The full-length *ASPM* gene contains 28 exons and encodes a spindle pole associated protein consisting of 3477 amino-acids, although alternatively spliced variants have also been detected (Kouprina et al., 2005, Létard et al., 2018). The main *ASPM* isoform contains an amino-terminal ASH (*ASPM*, *SPD-2*, *Hydin*) domain with a putative microtubule-binding function, an actin binding domain comprising two calponin homology (CH) domains, an IQ domain consisting of a series of repeated calmodulin-binding IQ (isoleucine-glutamine) motifs of variable length, an Armadillo-like domain, and a carboxyl-terminal region. This protein is conserved

between *Drosophila*, worm, mouse and human, with a consistent correlation of nervous system complexity and protein length, principally involving an increase in the number of calmodulin binding IQ motifs; the human protein displays 81 IQ motifs at positions 1273 to 3234. Calmodulin appears to regulate protein function by modulating its ability to bind to different targets either by altering the conformation of the protein or by influencing its subcellular location (Kouprina et al, 2005, Létard et al., 2018). More than 200 mutations, mostly nonsense or frameshift mutations, randomly distributed over the gene have been published so far. No genotype-phenotype correlation has been found (Létard et al., 2018).

The homozygous nonsense *ASPM* mutation [c.7323T>A, p.(Tyr2441Ter)] in exon 18, which creates a premature stop codon within the IQ domain (at repeat 49) in our patient has not been published yet. It may result either in unstable mRNA that would be degraded by nonsense-mediated RNA decay, or truncation of the protein at the calmodulin-binding IQ repeats domain. We did not perform functional studies to verify any of these mechanisms. Anyway, earlier studies on patients with *ASPM* mutations revealed the presence of truncated proteins indicating that the mutated *ASPM* mRNAs were not sensitive to nonsense-mediated RNA decay (Kouprina et al., 2005, Higgins et al., 2010). Majority of patients with *ASPM* mutations exhibit cerebral manifestations, but the somatic growth remains unaffected. It has been postulated, that either a functional compensatory mechanism exists in the somatic cells, or neurogenic cell divisions are sufficiently different from the somatic cell divisions being differently affected by disturbances of *ASPM* function (Higgins et al., 2010).

Simplified gyral pattern, corpus callosum anomalies, cerebellar and/or pontine hypoplasia have been reported as the most frequent cerebral anomalies in *ASPM*-related microcephaly (Bond et al., 2002, Bond et al., 2003, Woods et al., 2005, Létard et al., 2018). In contrast to these findings, our patient showed very severe cortical dysplasia with features of polymicrogyria. Our search of the literature revealed only a single patient with similar malformation of cortical development in *ASPM* mutation in addition to another patient with unilateral polymicrogyria (Passemar et al., 2009, Létard et al., 2018). We can hypothesize that modifying factors, still unknown, contributed to the development of this serious cortical malformation.

The human ***WDR62*** gene maps to chromosome 19q13.12, consists of 32 exons and encodes a 1523 amino acid protein containing several WD40 repeats (Shohayeb et al., 2018). More than 30 pathogenic mutations in *WDR62* have already been published. The frameshifts, missense, nonsense and splice site mutations in the *WDR62* gene are

randomly distributed. In addition to microcephaly, a wide range of malformations, including pachygyria, cortical thickening, cortical dysplasia, heterotopia, polymicrogyria, schizencephaly, dysmorphic hippocampus, corpus callosum abnormalities and cerebellar hypoplasia was described in these patients (Shohayeb et al., 2018). Neuropathology in a fetus with *WDR62* mutation revealed severe disruption of cortical neuronal architecture, immature radial columnar organization, and heterotopia in the intermediate zone (Yu et al., 2010).

We found diffuse pachygyria, thickened cortex and indistinct grey-white matter junction in our two patients from related families with the same novel homozygous missense *WDR62* mutation [c.668T>C, p.(Phe223Ser)]. This mutation affects one of the WD40 repeat regions of the *WDR62* protein. WD40 repeat is a short structural motif of approximately 40 amino acids, often terminating in a tryptophan-aspartic acid (W-D) dipeptide. The common function of all WD40 repeat proteins is coordinating multiprotein complex assemblies, where the repeating units serve as a rigid scaffold for protein interactions (Li and Roberts, 2001, Stirniman et al., 2010).

Experimental data on *Aspm*

In embryonic mice *Aspm* protein was highly expressed in the neuroepithelial cells when symmetric, proliferative divisions prevailed and declined progressively at later stages of neurogenesis (Bond et al., 2002, Fish et al., 2006, Capecchi and Pozner, 2015). It was recruited to the pericentriolar matrix at the spindle pole (Fish et al., 2006). *Aspm* by interacting with citron kinase exerted a critical role at the spindle poles of neuroepithelial cells in maintaining spindle axis exactly perpendicular to the neuroepithelial cell apical-basal axis throughout mitosis and, consequently, in ensuring the precise cleavage plane orientation required for symmetric, proliferative divisions (Fish et al., 2006, Gai et al., 2016). Loss of *Aspm* in knockdown mice resulted in deviation of spindle position, hence increasing the probability of asymmetric division of neuroepithelial cells, causing reduced expansion of neuroepithelial pool and leading to primary microcephaly (Fish et al., 2006, Fish et al., 2008, Gai et al., 2016).

Recent investigations revealed that ASPM has a mitotic orientation-independent effect on cell cycle duration. Regardless of division orientation, if the G1-phase of the cell cycle is sufficiently long for the cell to receive and process intrinsic or extrinsic differentiating signals, then the daughter cells will exit the cell cycle. ASPM by interaction with the Cdk2/Cyclin E complex regulates numerous aspects of the cell cycle progression, including mitosis duration and passage through the G1 restriction point

(Dehay and Kennedy, 2007, Capecchi and Pozner, 2015). Indeed, it has been shown in *Aspm* mutant mice that the cell cycle of the neural progenitor cells was prolonged. Especially, significant lengthening of the transition from the early G1 phase of the cell cycle to late G1 through the restriction point was observed, presumably promoting asymmetric division of the neural progenitor cells (Dehay and Kennedy, 2007, Capecchi and Pozner, 2015).

Experiments in *Aspm* knockout ferret, a species with a larger gyrified cortex and greater neural progenitor cell diversity than mice, basically confirmed a few aspects of *Aspm* function described in mice. A very large premature displacement (delamination) of ventricular radial glia cells (a type of neural progenitor cells) to the outer subventricular zone was observed in *Aspm* knockout ferret. Many of these cells resembled outer radial glia, a subtype of neural progenitor cells that are essentially absent in mice and have been implicated in cerebral cortical expansion in primates. These data suggested that *Aspm* regulates cortical expansion by controlling the affinity of ventricular radial glial cells for the ventricular surface, thus modulating the ratio of ventricular radial glial cells, the most undifferentiated cell type, to outer radial glia, a more differentiated progenitor (Fish et al., 2008, Johnson et al., 2018).

Experimental data on *Wdr62*

In vitro tests on cells with *WDR62/Wdr62* mutations and *in vivo* experiments in mice with knockdown or genetic inactivation of *Wdr62* showed similarities to the abnormalities found in patients with *ASPM* mutations and mice with *Aspm* knockdown (Shohayeb et al., 2018). The regulation and subcellular localization of WDR62 was found also to be cell cycle dependent. WDR62 protein accumulated strongly at the spindle poles during mitosis and showed cytosolic distribution in the interphase (Yu et al., 2010, Nicholas et al., 2010, Bogoyevitch et al., 2012, Farag et al., 2013, Sgourdou et al., 2017). Fibroblasts from a patient with homozygous *WDR62* mutation, or cells transfected with missense and frameshift *WDR62* mutations failed to show protein expression at the spindle poles (Nicholas et al., 2010, Farag et al., 2013, Sgourdou et al., 2017). *In vivo* experiments showed impaired proliferation of neocortical progenitors, reduced cortical thickness and small brain (Bogoyevitch et al., 2012, Chen et al., 2014, Jayaraman et al., 2016, Sgourdou et al., 2017). Abnormalities in the centriole duplication, spindle pole orientation, symmetric/asymmetric division of neural progenitor cells, defects in the mitotic progression, and premature delamination were noticed (Bogoyevitch et al., 2012, Chen et al., 2014). Increased apoptosis was also suggested as the cause of reduced brain

size (Bilgüvar et al., 2010, Nicholas et al., 2010, Yu et al., 2010, Bogoyevitch et al., 2012, Farag et al., 2013, Chen et al., 2014, Jayaraman et al., 2016, Sgourdou et al., 2017).

Recent studies revealed even more details of the premature depletion of progenitor cells and mitotic progression defects in mice with truncated *Wdr62* transcripts (*Wdr62*^{1-21/1-21}) (Sgourdou et al., 2017). As discussed above, centrosomes with differently aged mother centrioles are differentially inherited by the two daughter cells of asymmetrically dividing radial glia progenitors in the developing neocortex. WDR62 loss in mutant *Wdr62*^{1-21/1-21} mice disrupted asymmetric centrosome inheritance: the percentage of centrosomes retaining the old mother centriole decreased in the proliferating zones, while the percentage of centrosomes with new mother centrioles increased. The opposite was found in the cortical plate suggesting abnormal migration and possibly differentiation. This disturbed asymmetric centrosome inheritance may lead to impairment of mitotic cycle progression, premature depletion of progenitor cells from the ventricular zone, neuronal migration delay, altered neuronal differentiation and microcephaly eventually (Sgourdou et al., 2017).

As already mentioned, the Chromosome Passenger Complex is a major regulator of mitosis. It has been demonstrated that a fraction of WDR62 protein transiently co-localizes with Aurora kinase B as well as Survivin during mitosis. WDR62 disruption caused a decrease in centromere levels of Aurora B kinase at prophase, and a significant increase in levels of survivin at metaphase in fibroblasts from a patient with homozygous Asp955AlafsTer112 mutation in *WDR62* suggesting perturbed kinetochore function (Sgourdou et al., 2017).

Experimental data on *Aspm* and *Wdr62* interaction

Aspm and *Wdr62* proteins share common localization during the interphase at the mother centrioles. It has been shown that *Wdr62* is required to localize *Aspm* and other microcephaly-associated proteins to the centrosome. Mouse embryonic fibroblasts deficient in *Aspm*, *Wdr62*, or both show centriole duplication defects. It seems likely that centriole number and organization are critical for progenitor attachment to the ventricular surface and the maintenance of neural progenitors. Contrary to previous observations, it has been hypothesised recently that centriole duplication defect rather than premature asymmetric mitotic spindle orientation might be the major factor leading to depletion of progenitor cells resulting in microcephaly (Jayaraman et al., 2016, Jayaraman et al., 2018).

Taken together the experimental data provided some insight into the role of *Aspm/ASPM* and *Wdr62/WDR62* function in the development of brain size, however failed to clarify the precise mechanism of the wide range of structural abnormalities.

MEGALENCEPHALY

***FOXP1* gene**

FOXP1 (forkhead box protein P1; OMIM 605515) belongs to the functionally diverse family of forkhead (FOX) transcription factor proteins. It is one of four members of the *FOXP* subfamily (*FOXP1-4*) and acts as a transcriptional repressor (Wang et al., 2003, Golson and Kaestner, 2016). The *FOXP1* gene is located on chromosome 3p13 and consists of 16 exons coding for a protein with four tissue-specific, alternatively spliced isoforms. The *FOXP1* protein (Fig. 11 A), in addition to the forkhead/winged helix DNA-binding domain (FOX), possesses a leucine zipper motif, a zinc finger domain and an N-terminal polyglutamine (Q-rich) stretch (Wang et al., 2003, Meerschaut et al., 2017). The leucine zipper and zinc finger domains promote homodimerization and heterodimerization to the other *FOXP* family members, which is essential for DNA binding and transcriptional regulation. The N-terminal polyglutamine tract modulates the transcriptional repression activity of *FOXP1* (Li et al., 2004).

Monogenic *FOXP1* pathogenic variants (missense, nonsense, splice site mutations, deletions, or frameshifts), or more extensive 3p chromosomal deletions encompassing *FOXP1* have been reported previously in approximately 50 patients. No specific genotype-phenotype correlation was found (Hamdan et al., 2010, LeFevre et al., 2013, Meerschaut et al., 2017). A *FOXP1* mutation-related phenotype (OMIM 613670) as a recognizable entity has been outlined with intellectual disability, specific language impairment with or without autistic spectrum disorder and dysmorphic features (LeFevre et al., 2013, Meerschaut et al., 2017). The c.1573C>T, p.(Arg525Ter) heterozygous nonsense *de novo FOXP1* mutation in our patient causes premature truncation of the protein in the winged-helix evolutionally conserved DNA-binding (FOX) domain by abolishing the last 152 amino acids of *FOXP1*. *In vitro* functional characterization of *FOXP1* variants provided evidence that this mutation was pathogenic (Sollis et al., 2016, Meerschaut et al., 2017). Direct fluorescence imaging studies showed that the wild type protein was localized to the nuclei, excluded from the nucleoli, while the p.Arg525Ter variant was excluded from the nuclei and formed large cytoplasmic aggregate suggesting misfolding of the aberrant protein (Sollis et al., 2016). In addition, the variant lost its

transcriptional repressive activity pointing to disturbance of transcription regulation (Hamdan et al., 2010, Sollis et al., 2016, Meerschaut et al., 2017). FOXP proteins regulate gene expression by forming homo- and hetero-dimers with each other and they interact with other transcription factors forming a network involved in cortical development (Estruch et al., 2018). Protein interaction studies revealed that the p.Arg525Ter variant did not interact with wild type FOXP1/FOXP2 and was unable to self-associate, likely because of misfolding (Sollis et al., 2016). *In vivo*, however, it is possible that the nonsense mutation results in nonsense-mediated mRNA decay.

Experimental data on *FOXPI*

The precise functions of FOXP1 transcription factor in brain development remained unclear so far. FOXP1/*Foxp1* was found to be expressed in the developing cerebral cortex in humans and experimental animals following neuronal migration suggesting a role for this gene in neuronal differentiation (Ferland et al., 2003, Teramitsu et al., 2004).

Homozygous loss of *Foxp1* in all tissues was embryonically lethal in mice because of cardiac defect (Wang et al., 2003). Brain specific homozygous *Foxp1* deletion resulted in viable offspring with postnatal reduction of the dorsal and enlargement of the ventral regions of the striatum. These animals displayed reduced excitability in the CA1 hippocampal pyramidal neurons and showed developmental delay in association with impaired behavior (Bacon et al., 2015). It is noteworthy that an increase in the total brain volume, or abnormalities of the corpus callosum were not described in these mutant mice. Recently, neuronal migration defect with ectopic neurons in deep layers of the cortex have been found in mice following down-regulation of *Foxp1* expression in the cerebral cortex (Li et al, 2015). Migration, or cortical lamination defect were not seen in our patient by conventional MRI; however, it could not be excluded at histological level, beyond the scope of MRI resolution. Dendritic spine dysgenesis appeared to be a common finding in individuals with intellectual disability and autism-related disorders [Phillips et al., 2015] and indeed, it might be responsible for the severe intellectual disability in our patient.

***PTCHI* gene**

The *PTCHI* gene on chromosome 9q22.3 is a human homolog of the *Drosophila* segment polarity gene, patched (*patched homolog 1*, OMIM 601309; *ptc*, or *Patched1* in some of the publications on rodents) and consists of 23 exons (Hahn et al., 1996, Lindström et al., 2006). It encodes a transmembrane glycoprotein (Fig. 11 B) composed

of 1447 amino acids with 12 transmembrane regions, an intracellular and two extracellular loops, and a putative sterol-sensing domain (Hahn et al., 1996, Lindström et al., 2006). It functions as a sonic hedgehog (SHH) receptor and regulates SHH signaling at the primary cilium (Marigo et al., 1996, Rohatgi et al., 2007, Briscoe and Théron, 2013). SHH has an important role in embryonic development by establishing cell fate in the neural tube, somites, and limbs. (Briscoe and Théron, 2013, Jia et al., 2015, Pellegrini et al., 2017). In the absence of SHH, PTCH1 represses the function of the seven-pass transmembrane protein, Smoothed (SMO). SHH binding to PTCH1 inhibits this repression of SMO, which results in the activation of the GLI (Glioblastoma-associated oncogene) family transcription factors (Rohatgi et al., 2007, Briscoe and Théron, 2013, Gong et al., 2018) (Fig. 11 C).

Heterozygous germline *PTCH1* mutations cause Gorlin syndrome (OMIM 109400, Gorlin-Goltz syndrome, nevoid basal cell carcinoma, or basal cell nevus syndrome), an autosomal dominant disorder that predisposes affected individuals to developmental defects and tumorigenesis (Kimonis et al., 1997, Gorlin 2004, Pellegrini et al., 2017). Dozens of pathogenic variants in the *PTCH1* gene include deletions or insertions, (multi)exon or large-scale deletions or rearrangements resulting in frameshifts, nonsense mutations leading to premature stops, missense, splice-site mutations, and deep intronic variants that alter splicing (Hahn et al., 1996, Lindström et al., 2006, Gianferante et al., 2018). A careful analysis revealed that high frequency of mutations is clustered into the intracellular and two extracellular loops (Lindström et al., 2006). Indeed, the p.(Arg945GlnfsTer22) in our patient affects one of the extracellular loops (Fig. 11 B), leading to protein truncation, or nonsense-mediated mRNA decay. Either way, the attachment of SHH to the receptor PTCH1 and the suppression of SMO by PTCH1 might be impaired resulting in dysregulation of the SHH signaling pathway.

Experimental data on *PTCH1* (*patched homolog 1*)

Consistent with the role of Shh in brain development, patched homolog 1 (Ptc1, PTCH1) the putative receptor for Shh protein plays also an important role in neural development. Experimental studies showed expression of Ptc1 protein throughout the mouse embryo. It was bound to Shh and other hedgehog family members and formed a complex with Smo (Carpenter et al., 1998). Mice homozygous for the Patched mutation (*Ptc*^{-/-}) died during embryogenesis and were found to have open and overgrown neural tubes (Goodrich et al., 1997). Mice heterozygous for the *Ptc* mutation were larger than normal, and a subset of them developed hindlimb defects or cerebellar medulloblastoma

(Goodrich et al., 1997). These studies suggest that the balance between hedgehog and Ptc activities appears critical for normal development and neural fate determination (Goodrich et al., 1997).

The role of *PTCH1* in oncogenesis

Experiments revealed that inactivation of the *Ptc* gene either in cerebellar granule neuron precursors or multipotent neural stem cells led to Shh pathway activation and medulloblastoma (Yang et al., 2008). Patients with *PTCH1* mutations have high risk of medulloblastoma and/or basal cell carcinoma due to SMO activation and increased transcription of SHH-pathway target genes (Pellegrini et al., 2017). Medulloblastoma is the most common malignant paediatric brain cancer and comprises four major subgroups [Sonic hedgehog (SHH), WNT, group 3, and group 4]. Proliferation of cerebellar granule cell precursors that give rise to SHH-medulloblastoma is regulated by SHH signalling during the third trimester to the first few months of life in human. Most of the SHH-medulloblastoma samples have mutations in four genes that lead to SHH pathway activation: loss of function mutations in two genes that inhibit the SHH pathway [Patched1 (*PTCH1*) and *SUFU*], activating mutations in Smoothed (SMO), and *TP53* loss associated with amplification of *GLI2* or *NMYC* that act downstream of SHH (Tan et al., 2018). Interestingly, the lateral cerebellum is preferentially sensitive to high sonic hedgehog signalling and 59% of tumours with *PTCH1* mutation develop in the cerebellar hemispheres (Tan et al., 2018).

Coexistence of *FOXPI* and *PTCH1* mutations

Heterozygous disruptions in both *FOXPI* and *PTCH1* genes were found in our patient with extreme megalencephaly, partial callosal agenesis and profound intellectual disability. Common and distinct features described either in *FOXPI* or *PTCH1* mutations could be recognized (Table 2). Several clinical characteristics of Gorlin syndrome, like basal cell carcinoma, multiple jaw keratocysts, cardiac and ovarian fibromas were lacking, but these features have age-dependent manifestation, and their presence in a child would not be expected (Veenstra-Knol et al., 2005, Kimonis et al., 2013). Facial milia and skeletal abnormalities were not observed and medulloblastoma did not develop until the last follow-up. (Gorlin, 2004, Kimonis et al., 2004, Veenstra-Knol et al., 2005).

A tendency to head circumference above mean and megalencephaly have been described either in *FOXPI*-, or *PTCH1*-related conditions, however, such an extreme rate of head growth, as seen in our patient has never been reported in association with disease-causing variants in these genes (Kimonis et al., 1997, Hamdan et al., 2010, LeFevre et al.,

2013, Kimonis et al., 2013, Fuji K et al., 2014, Meerschaut et al., 2017). Although structural brain abnormalities have been found occasionally in *FOXP1*-related disorders, corpus callosum malformation has not been reported (Meerschaut et al, 2017). Brain malformations were also rarely reported in association with *PTCH1* mutations: partial or complete agenesis of the corpus callosum was found only in a few cases (Kimonis et al., 1997, Takanashi et al., 2000, Kimonis et al., 2004, Veenstra-Knol et al., 2005, Mazzuocolo et al., 2014, Morita et al., 2015). Recently, however, volumetry has revealed reduced callosal thickness in association with enlarged hemispherical and cerebellar diameters in children with *PTCH1* mutations and nevoid basal cell carcinoma (Shiohama et al., 2017). It seems that the intellectual disability and language deficit were less severe in children with mutations only in one of these genes (Kimonis et al., 2013, Meerschaut et al., 2017). *We suggest that the effects of multiple hits, disruptive disease-causing variants in two different genes simultaneously added and resulted in the serious composite clinical phenotype in our patient. FOXP1 mutation might contribute to the severe intellectual disability, while the extreme megalencephaly in association with the partial callosal agenesis might rather be related to the PTCH1 mutation (Table 2).* Further studies on possible functional interactions between the two genes may clarify the molecular basis of this phenotype.

Activating mutations in the PI3K (phosphatidylinositol-3-kinase) – AKT (AK mouse + Transforming or Thymoma) -mTOR pathway and megalencephaly.

Mutations of upstream (*PIK3R2*, *PIK3CA*, *PTEN*), central (*AKT3*, *TSC1*, *TSC2*, *MTOR*, *DEPDC5*) and downstream (*CCND2*) genes within the PI3K-AKT-mTOR pathway are associated with brain overgrowth (megalencephaly), as well as cortical dysplasia (such as hemimegalencephaly, focal cortical dysplasia and polymicrogyria). Mutations in these genes lead to activation of the PI3K-AKT-mTOR pathway (Mirzaa et al., 2013, Mirzaa et al., 2016, D’Gama et al., 2017).

The PI3Ks are members of a unique and highly conserved family of intracellular lipid kinases that phosphorylate the 3'-hydroxyl group of phosphatidylinositol and phosphoinositides, a reaction that leads to the activation of many complex intracellular signalling pathways including the PI3K-AKT-mTOR network. These signalling enzymes regulate a wide range of processes, including cell growth, proliferation, survival, migration, metabolism, angiogenesis, apoptosis, tumorigenesis and brain development (Cohen, 2013, Engelman et al., 2006, Manning and Toker, 2017).

There are three classes (I-III) of PI3Ks according to their substrate preferences and sequence homology. Class I PI3Ks are divided into two subfamilies, depending on the receptors to which they couple. Class IA PI3Ks are activated by growth factor receptor tyrosine kinases (RTKs, Fig. 12), whereas class IB PI3Ks are activated by G-protein-coupled receptors (Cohen, 2013, Engelman et al., 2006, Fig. 12 B)). Gene mutations, described so far as responsible for megalencephaly, affect subunits of class IA PI3Ks.

Class IA PI3Ks are composed of heterodimers of p110 catalytic and p85 regulatory subunits (Fig. 12), each of which has several isoforms encoded by three genes. Three genes - *PIK3CA*, *PIK3CB*, and *PIK3CD* - encode the highly homologous p110 catalytic subunit isoforms p110 α , p110 β , and p110 δ , respectively. (Cohen, 2013, Engelman et al., 2006). Three genes, *PIK3R1*, *PIK3R2* and *PIK3R3* encode the p85 α , p85 β and p85 γ isoforms of the p85 regulatory subunit, respectively. The class IA p85 regulatory isoforms have a common core structure consisting of a p110-binding domain flanked by two Src-homology 2 (SH2) domains. The p85 regulatory subunit is crucial in mediating the activation of class IA PI3K by receptor tyrosine kinases (RTKs, Cohen, 2013, Engelman et al., 2006) (Fig 12).

AKT is the most widely studied effector of PI3K signalling. There are three isoforms (Figs. 10 A, 12); AKT1 and AKT2 isoforms are ubiquitously expressed, whereas the AKT3 isoform is mainly expressed in the brain and testis. (Cohen, 2013, Manning and Toker, 2017). Each of the AKT isoforms contains a pleckstrin homology domain (PH, amino acids 5-107 in AKT3) in the N-terminal region followed by the linker region (amino acids 107-148 in AKT3) connecting the PH domain to the kinase (catalytic) domain (amino acids 148-405 in AKT3) and the regulatory C-terminal region (amino acids 406-479 in AKT3) (Figs. 10 A, 12). Pleckstrin is a protein found in platelets and its name stands for **p**latelet and **l**eukocyte **C** kinase substrate and the KSTR string of amino acids. (Cohen, 2013, Manning and Toker, 2017). All three AKT isoforms undergo membrane recruitment through the N-terminus PH domain which binds to PIP₃ and the inactive forms of the AKTs become activated by this attachment (Cohen, 2013, Manning and Toker 2017) (Fig 12). The chromosomal localization of the three genes encoding the AKT isoforms are as follows: *AKT1* on chromosome 14q32.3 (OMIM 164730), *AKT2* on chromosome 19q13.2 (OMIM 164731), and *AKT3* on chromosome 1q43-q44 (OMIM 611223) (Fig 10 A).

The activity of the PI3K can be assessed by immunostaining to compare PIP₃ amounts in lymphoblastoid cell lines derived from mutation carriers with megalencephaly

to those in controls (Rivière et al., 2012). The activation state of kinases in the PI3K-AKT-mTOR pathway can be examined through the use of antibodies specific for the phosphorylated forms of their target proteins. Phosphorylation of the downstream targets, such as ribosomal protein S6 and eukaryotic translation initiation factor 4E-binding protein 1 (4E-BP1) reflects the activation at any level of the PI3K-AKT-mTOR pathway (Engelman et al., 2006, Lee et al., 2012, Jansen et al., 2015, Biever et al., 2015, Qin et al., 2016).

AKT3 gene

Mutations in *AKT3* are responsible for *megalencephaly-polymicrogyria-polydactyly-hydrocephalus syndrome 2; MPPH2, OMIM 615937*). *AKT3* consists of 24 exons and 479 amino acids. Mutations of *AKT1* and *AKT2* have been identified in somatic overgrowth disorders such as Proteus syndrome (Lindhurst et al., 2011) and in somatic overgrowth with hypoglycaemia (Hussain et al., 2011), respectively.

At first, copy number changes suggested a role of *AKT3* in brain size control. In hemimegalencephaly and focal cortical dysplasia mosaic somatic partial 1q trisomy and mosaic somatic trisomy of the 1q21.1-q44 chromosomal region were found in surgically removed tissue. These regions encompassed the *AKT3* gene (Poduri et al., 2012; Conti et al., 2015). Germline duplication of 1q43q44 that included *AKT3* was associated with megalencephaly probably due to dosage imbalance (Wang et al., 2013; Chung et al., 2014; Hemming et al., 2016). In contrast, microdeletions of 1q43q44 regions were associated with microcephaly, suggesting that haploinsufficiency of this gene might be responsible for this phenotype (Ballif et al., 2012; Gai et al., 2015; Hemming et al., 2016; Depienne et al., 2017).

Before 2017 a few *constitutional* mutations of *AKT3* in association with megalencephaly and polymicrogyria and several *mosaic* mutations in hemimegalencephaly were reported (Riviere et al., 2012; Lee et al., 2012; Januar et al., 2014; Nakamura et al., 2014; Jansen et al., 2015; Harada et al., 2015; Nellist et al., 2015; Takagi et al.; 2017; Negishi et al., 2017). *Eventually* the wide spectrum of developmental disorders found in 11 children reported previously and 14 newly diagnosed individuals with either constitutional or mosaic mutations in *AKT3* have been reviewed (Alcantara D et al., 2017). Patients with constitutional mutations have been segregated into three groups, such as (i) *megalencephaly-polymicrogyria, including our patient*, (ii) megalencephaly-polymicrogyria with periventricular heterotopia, and finally (iii) megalencephaly with no or subtle cortical malformation and autism spectrum disorder

(Nellist et al., 2015; Takagi et al., 2017; Alcantara et al., 2017). Therefore the phenotype associated with *AKT3* mutations proved to be wider than the megalencephaly-polymicrogyria-polydactyly-hydrocephalus syndrome 2 as suggested in the OMIM.

The moderate dilatation of the lateral ventricles in our patient did not require surgical intervention. Polydactyly was not observed, just partial syndactyly of the toes. Epilepsy with varying severity was described in *AKT3* mutations; the seizure disorder was mild and easily controlled in our patient. The global developmental delay was severe, corresponding to the extended cortical dysgenesis. Patchy capillary vascular malformations, hypoglycaemia (Nellist et al., 2015, Alcantara et al., 2017), and growth hormone deficiency (Takagi et al., 2017) were reported in association with *AKT3* mutations, however they were absent in our patient.

The constitutional *de novo* heterozygous missense variant, c.1393C>T, p.(Arg465Trp), found in our patient was published only in 7 individuals (Fig. 10 B) so far (Rivière et al., 2012; Jamuar et al., 2014; Alcantara et al., 2017). It localizes to a CpG site in the C-terminal region of *AKT3* (Pfeifer, 2006, Rivière et al., 2012,) (Fig 10. A, B).

Activated AKT phosphorylates downstream substrates either to activate, or more often inhibit the function of proteins that are involved in the regulation of diverse cellular functions, such as metabolism, translation, proliferation, survival, and angiogenesis (Engelman et al., 2006, Cohen, 2013, Manning and Toker 2017). The three best-established downstream targets of AKT include glycogen synthase kinase 3 (GSK3), forkhead box O (FOXO) transcription factors and tuberous sclerosis complex 2/mammalian target of rapamycin complex 1 (TSC2/mTORC1). The latter group of targets have the most relevance to paediatric neurology. The regulation of cell and tissue growth is primarily through the AKT-mediated activation of the protein kinase complex mTORC1, which stimulates cell growth. The tuberous sclerosis complex (TSC) a protein complex containing TSC1, TSC2 and TBC1D7 is a potent inhibitor of mTORC1. The AKT-mediated phosphorylation of TSC2 relieves this inhibition to activate mTORC (Engelman et al., 2006, Cohen, 2013, Manning and Toker 2017).

Experimental data on *AKT3* gene

AKT3 protein is phosphorylated on Thr305 by 3-phosphoinositide-dependent protein kinase 1 (PDK1) and on Ser472 by the mTORC2 complex (Fig 12). Phosphorylation of AKT at both sites is required for full kinase activity (Manning and Toker, 2017). As already mentioned above, phosphorylation of ribosomal protein S6 serves as a downstream readout of activation at any level of the PI3K-AKT-mTOR

pathway. It was demonstrated that cells with the morphology of cytomegalic neurons in hemimegalencephaly due to mosaic *AKT3* mutation [c.49G>A, p.(Glu17Lys)] were strongly labelled for phosphorylated S6, suggesting gain of function in the PI3K-AKT-mTOR pathway (Lee et al., 2012). Further experiments on surgical brain tissue from hemimegalencephaly, - including a specimen with mosaic *AKT3* mutation [(c.49G>A, p.(Glu17Lys)), - and focal cortical dysplasia interestingly exhibited an activation of phosphorylation in both the threonine and serine sites of AKT protein regardless of the presence or absence of detected PI3K-AKT-mTOR pathway mutations. Patients with negative sequencing results either may have mutations of other genes, influencing the PI3K-AKT-mTOR pathway, very low level mosaic mutations below the detection limit, or aberrant activation of the pathway through other mechanism (Jansen et al., 2015). Increased immunosignal was found for antibodies against phosphorylated ribosomal protein S6, AKT, its activated, phosphorylated form (pAKT), mTOR, PI3K (p110 α), PTEN and phosphor-PDK1 also in the brain tissue of a patient with focal cortical dysplasia in association with mosaic somatic 1q21.1-q44 duplication, including duplication of the *AKT3* gene (Conti et al., 2015).

In other experiments there was no evidence for increased PI3K activity in the *AKT3*-mutant cell line, consistent with a mutation affecting a downstream effector of PI3K (Rivière et al., 2012). However, higher S6 and 4E-Bp1 phosphorylation was measured in a lymphoblastoid cell line harbouring the *AKT3* c.1393C>T; p.(Arg465Trp) alteration, strongly suggesting a gain-of-function mechanism resulting in enhanced *AKT3* activity (Rivière et al., 2012; Negishi et al., 2017). Kinase activity analysis also clearly showed that all mutations causing megalencephaly, including the constitutional variant, found in our patient caused increased activity compared to wild-type, confirming that these mutations are also activating the PI3K-AKT-mTOR pathway (Alcantara et al., 2017).

In accordance with the microdeletions of the 1q43q44 regions, encompassing the *AKT3* gene, animal studies revealed that mice lacking *Akt3* (*Akt3*^{-/-}) showed microcephaly secondary to both a decrease in cell number and reduction in cell size. (Easton et al., 2005; Tschopp et al., 2005). In addition ribosomal protein S6 phosphorylation was decreased by almost 50% in *Akt3* knockout brains. It seems that *Akt3* controls the mass of the mouse brain by influencing both cell size and number, most likely through the selective activation of downstream effectors in the PI3K-Akt-mTOR pathway (Easton et al., 2005). Seizures were not observed in these animals. On the

contrary, heterozygous, or homozygous missense mutation in mice leading to an amino acid substitution of aspartic acid to valine (Asp219Val) resulted in seizure susceptibility by decreasing the seizure threshold. An increased brain size, ectopic hippocampal neurons and enhanced kinase function of AKT3 were also observed in these animals. (Tokuda et al., 2011). Our patient with an activating mutation in *AKT3* also showed susceptibility to seizures, although the polymicrogyria itself may have intrinsic epileptogenicity (Kobayashi et al., 2005).

The PI3K–AKT–mTOR pathway in oncogenesis

The PI3K-AKT-mTOR pathway is one of the most commonly dysregulated pathways in all of cancer. Overexpression and/or mutations of genes encoding the tyrosine kinase receptors, or genes of the PI3K pathway represent some of the most common mutations in oncology (Cheung and Testa, 2013; Mundi et al., 2016). *AKT3* upregulation due to increased copy number of chromosomal region 1q44, where *AKT3* is located, was found in hepatitis C virus-associated hepatocellular carcinoma. Moreover 40-60% of primary melanomas were found to have increased total or phosphorylated AKT3 protein compared to normal melanocytes (Stahl et al., 2004; Cheung and Testa, 2013). AKT plays an important role in the maintenance of the homeostatic balance of cell division and growth on one hand, and programmed cell death on the other. Disruption of this balance may be responsible for tumorigenesis. The well characterized interactions of AKT make it a highly attractive target for cancer therapy (Cheung and Testa, 2013; Mundi et al., 2016). Considering the findings regarding the relationship between PI3K-AKT-mTOR pathway activation and oncogenesis careful monitoring of Patient 5 for cancer is warranted.

CONCLUSIONS

This study provides phenotypic and genotypic characterization of three patients with microcephaly and two patients with megalencephaly. Next generation sequencing revealed novel homozygous pathogenic variants in the *ASPM* and *WDR62* genes causing autosomal recessive primary microcephaly (MCPH). These mutations might lead to abnormal function of the centrosomes, which organize the separation of chromosome copies during cell division. Coexistence of heterozygous *de novo* variants in *FOXP1* and *PTCH1* genes was found in association with extreme megalencephaly and profound intellectual disability, as a composite phenotype, sharing some features of Gorlin syndrome. Activating heterozygous mutation in *AKT3*, a gene encoding a protein in the

PI3K-AKT-mTOR pathway resulted in megalencephaly and polymicrogyria. There is evidence that abnormalities in the PTCH1-SHH and PI3K-AKT-mTOR pathway have significant role in oncogenesis, therefore our patients with brain overgrowth require regular medical follow-up. Autosomal recessive primary microcephaly and megalencephaly are rare diseases and our study is in line with the international efforts of discovering the molecular background of these disorders.

ACKNOWLEDGEMENTS

I am grateful to László Sztriha, PhD, DSc, Professor Emeritus, my mentor, for his advices.

I thank Csaba Bereczki, PhD, Associate Professor, Chairman of the Department of Paediatrics, University of Szeged for his support.

I am grateful to Tibor Kalmár, PhD and Zoltán Maróti, PhD for their help.

I am grateful to my husband and my parents for their tolerance and support.

TABLES

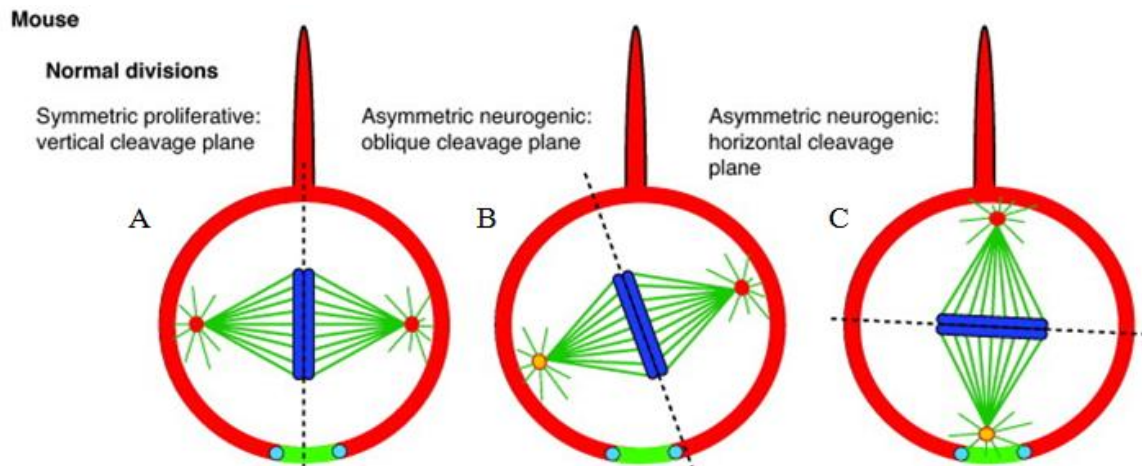
Table 1
Genes and mutations reported in this study

Patients	Genes	Exons	Nucleotide variation	Amino acid variation	Mutation type	Zygoty	Main phenotypic feature	Comments
1	<i>ASPM</i>	Exon 18	c.7323T>A	p.Tyr2441Ter	Nonsense	Homozygous	Microcephaly	Novel
2	<i>WDR62</i>	Exon 6	c.668T>C	p.Phe223Ser	Missense	Homozygous	Microcephaly	Novel
3	<i>WDR62</i>	Exon 6	c.668T>C	p.Phe223Ser	Missense	Homozygous	Microcephaly	Novel
4	<i>FOXP1</i> <i>PTCH1</i>	Exon 18 Exon 17	c.1573C>T c.2834delG insAGATGTTGT GGACCC	p.Arg525Ter p.Arg945Glnfs Ter22	Nonsense Frameshift	Heterozygous <i>de novo</i> Heterozygous <i>de novo</i>	Megalencephaly	Published Novel
5	<i>AKT3</i>	Exon 13	c.1393C>T	p.Arg465Trp	Missense	Heterozygous <i>de novo</i>	Megalencephaly	Published

Table 2
Common versus distinct clinical features attributable to mutations in *FOXP1* and *PTCH1*

	<i>FOXP1</i> (Le Fevre et al., 2013 Meerschaut et al., 2017)	<i>PTCH1</i> (Veenstra-Knol et al., 2005 Kimonis et al., 2013 Shiohama et al., 2017)
Head size	Megalencephaly	
Dysmorphic features	Prominent forehead Strabismus Broad nasal bridge	
	Frontal hair upsweep Down slanting palpebral fissures Short nose with broad tip Long philtrum Abnormally modelled ears	Highly arched eyebrows Low-set ears Symmetrical post-axial cutaneous appendages (skin tags) on both hands
Brain imaging		Partial agenesis of the corpus callosum Widely separated leaves of the septum pellucidum
	Enlarged cerebral ventricles	
Neurological signs	Global developmental delay Profound intellectual disability Generalized hypotonia	

FIGURES

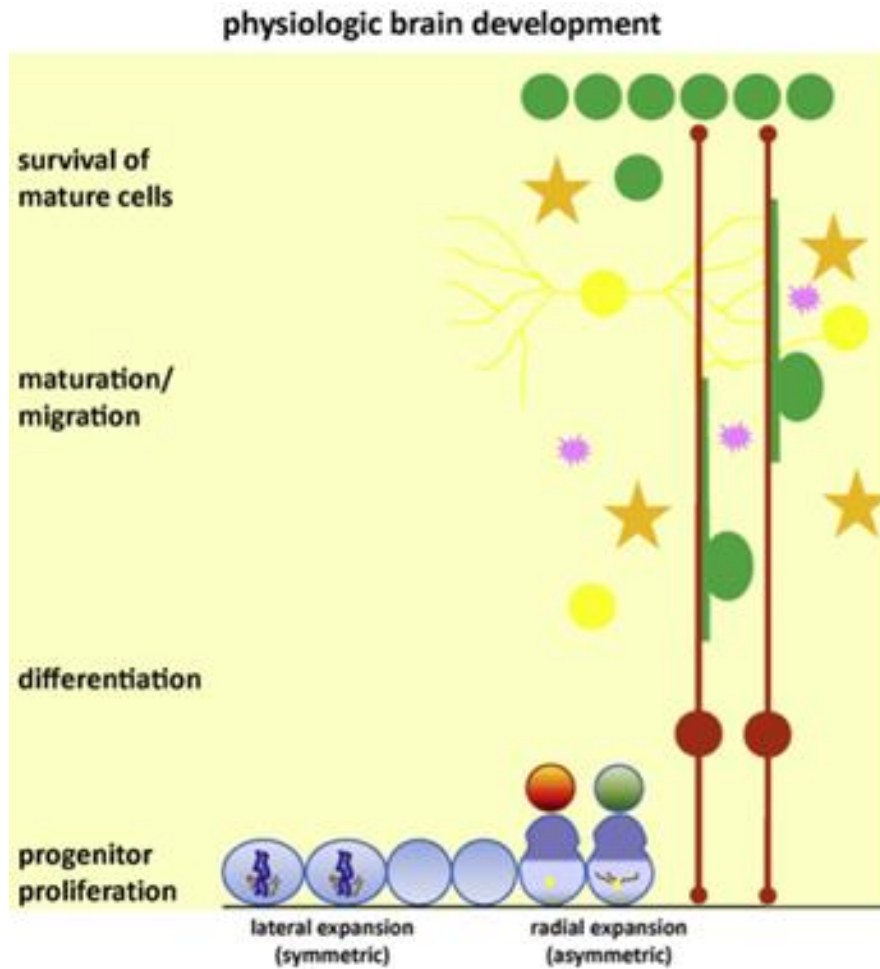
**Explanatory figure 1**

Centrosome regulation of neural progenitor proliferation

(A) Alignment of mitotic spindles parallel to the neuroepithelium within the progenitor cells results in symmetrical divisions and thereby an increase of the progenitor pool.

(B and C) An alignment of the spindle perpendicular to the neuroepithelium results in asymmetric cell divisions, which maintain the progenitor pool cell numbers while producing precursors of various cell types, such as neurons and glial cells.

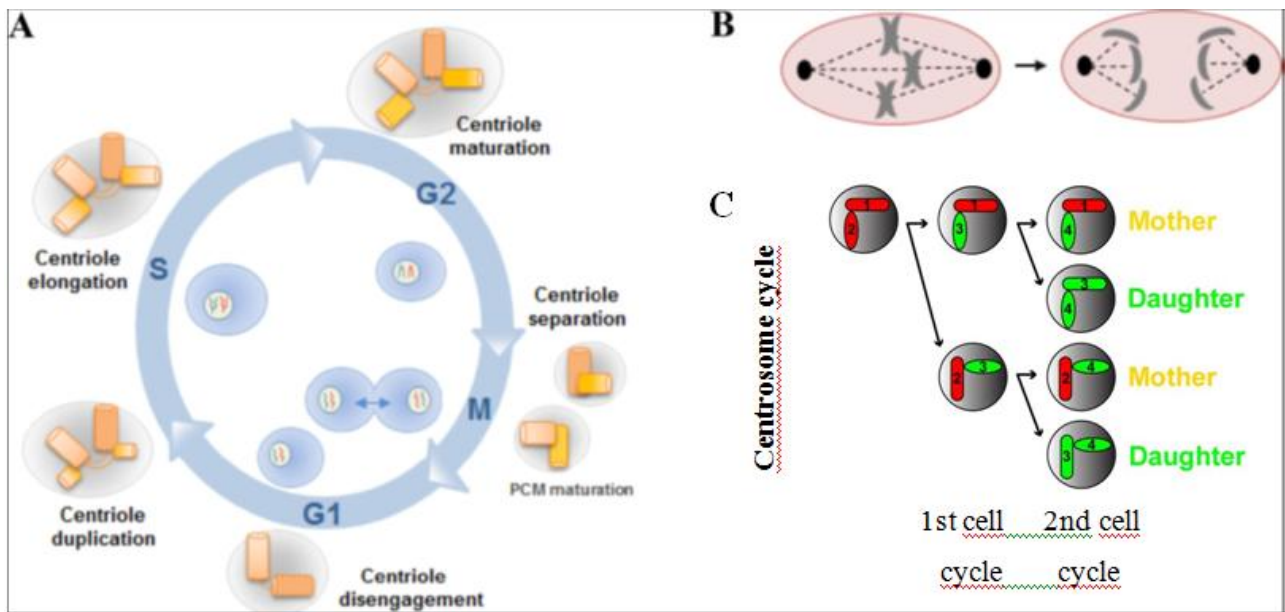
(Megraw L, Sharkey JT, Nowakowski RS. *Trends Cell Biol* 2011;21:470-480)



Explanatory figure 2

Neurons and glial cells further differentiate, mature and migrate.

(Kaindl AM et al. *Prog Neurobiol* 2010;90:363-383)

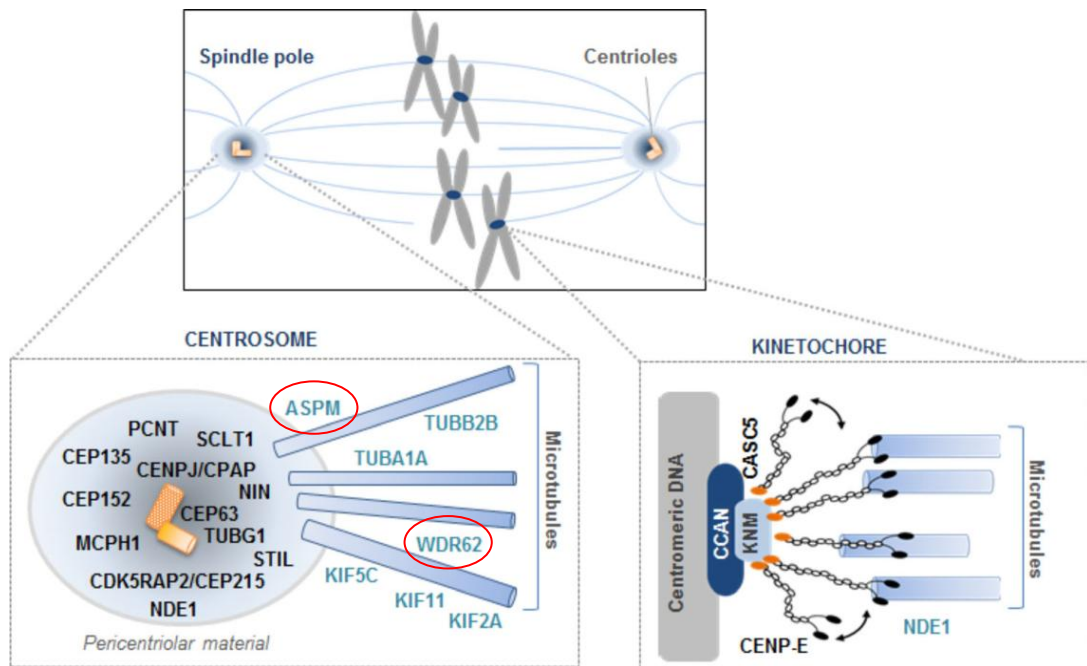


Explanatory figure 3

(A) The cell cycle of eukaryotic cells can be divided into four successive phases: M phase (mitosis), S phase (DNA synthesis) and two gap phases, G1 and G2. Centrosomes play an essential role in cell division, as they are responsible for the formation and maintenance of the microtubule-based spindle apparatus. The centrosome contains a pair of cylindrical centrioles in an orthogonal configuration. Centriole duplication occurs during each cell-cycle and both centrioles and centrosomes undergo final maturation in the G2 and M phases. (Prosser SL, Pelletier L. *Nat Rev Mol Cell Biol* 2017;18:187-201, Nigg EA, Holland AJ. *Nat Rev Mol Cell Biol* 2018;19:297-312, Alcantara D, O’Driscoll M, *Am J Med Gen Part C Semin Med Genet* 2014;166C:124–139)

(B) Centrosomal duplication results in the generation of a bipolar mitotic spindle. (Alcantara D, O’Driscoll M, *Am J Med Gen Part C Semin Med Genet* 2014;166C:124–139)

(C) Centrosome duplication in dividing neuroprogenitors generates a pair of centrosomes with differently aged mother centrioles. During peak phases of neurogenesis the centrosome retaining the old mother centriole stays in the ventricular zone and is preferentially inherited by neuroprogenitors, whereas the centrosome containing the new mother centriole mostly leaves the ventricular zone and is largely associated with differentiating cells. (Wang *et al. Nature* 2009;461:947-955)



Explanatory figure 4

The distribution of genetic defects underlying congenital microcephaly attributable to the centrosome, spindle and kinetochore. The upper panel depicts a normal bipolar mitosis.

In embryonic mice, Aspm protein was recruited to the pericentriolar matrix at the spindle pole. It ensured the precise cleavage plane orientation required for symmetric, proliferative divisions. Loss of Aspm resulted in deviation of spindle position, hence increasing the probability of asymmetric division of neuroepithelial cells, causing reduced expansion of neuroepithelial pool and leading to primary microcephaly.

WDR62 protein accumulated at the spindle poles during mitosis. Cells with WDR62 mutations failed to show protein expression at the spindle poles. Abnormalities in the centriole duplication, spindle pole orientation, symmetric/asymmetric division of the neuronal progenitor cells, defects in the mitotic progression, and premature delamination were noticed.

Experiments revealed that Aspm and Wdr62 proteins share common localization during the interphase at the mother centrioles. Wdr62 is required to localize Aspm and other microcephaly-associated proteins to the centrosome. Mouse embryonic fibroblasts deficient in Aspm, Wdr62 or both show centriole duplication defects. It seems likely that centriole number and organization are critical for neuronal progenitor attachment to the ventricular surface and the maintenance of neuronal progenitors. The centriole duplication defect might be the major factor leading to depletion of progenitor cells resulting in microcephaly. (Alcantara D. et al. *Am J Med Genet* 2014;166C:124-139)

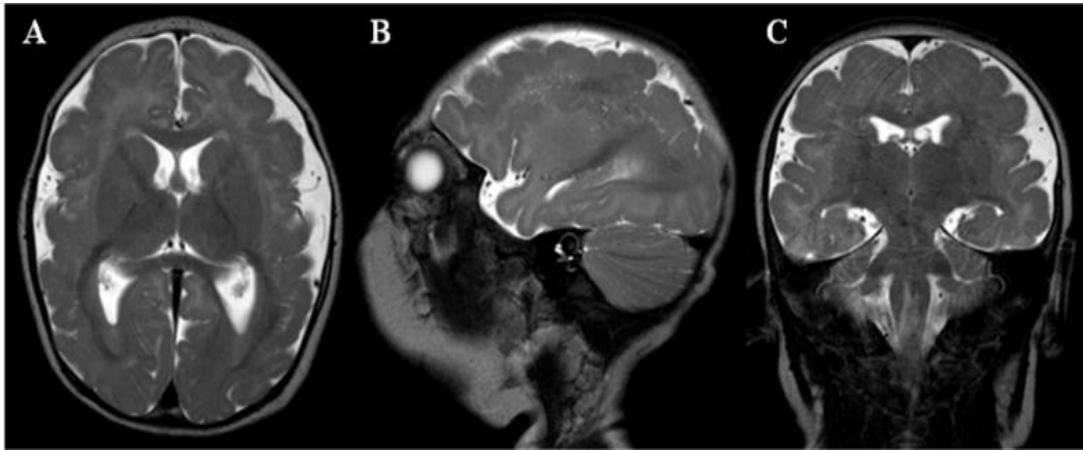


Fig. 1

Patient 1. Brain MRI. T2 weighted axial (A), parasagittal (B) and coronal (C) images at age of 7 months. The architecture of the cortex is abnormal, features of dysplasia and polymicrogyria can be seen. The grey-white matter junction appears indistinct at some areas. The Virchow-Robin spaces and lateral ventricles are dilated.

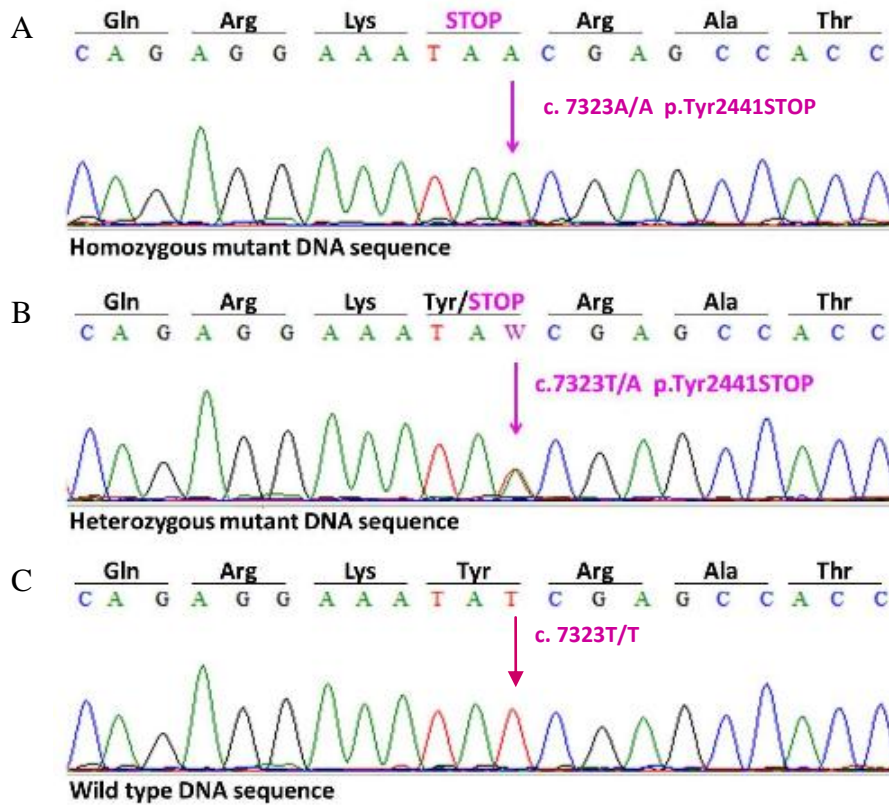


Fig. 2.

Patient 1. Sanger sequencing of part of exon 18 of the *ASPM* gene shows the homozygous T to A mutation at position 7323 of the coding DNA sequence (A). This variant creates a premature stop codon. The mutation is heterozygous in the parents (B). The 7323 positions are indicated by arrows. A normal sequence is also shown in an unrelated control subject. (C).

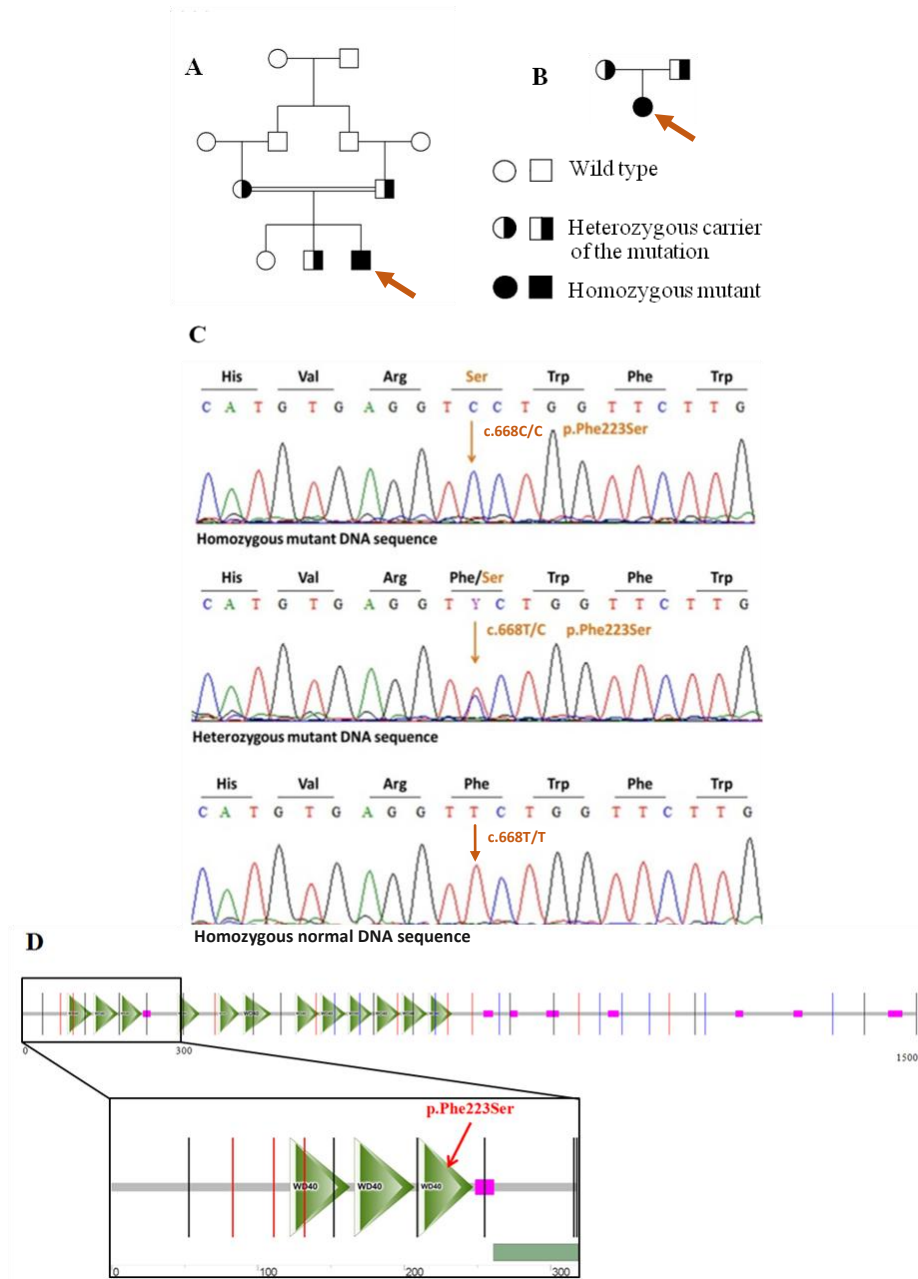


Fig. 3

Pedigree of Patient 2 (**A**) and Patient 3 (**B**). Sanger sequencing of part of exon 6 of the *WDR62* gene shows the homozygous T to C mutation at position 668 of the coding DNA sequence (**C**, arrows). The mutation is heterozygous in the parents and brother of Patient 1. A normal sequence is also shown in an unrelated control subject (**C**). The mutation affects one of the WD40 repeats in the WDR62 protein (**D**).

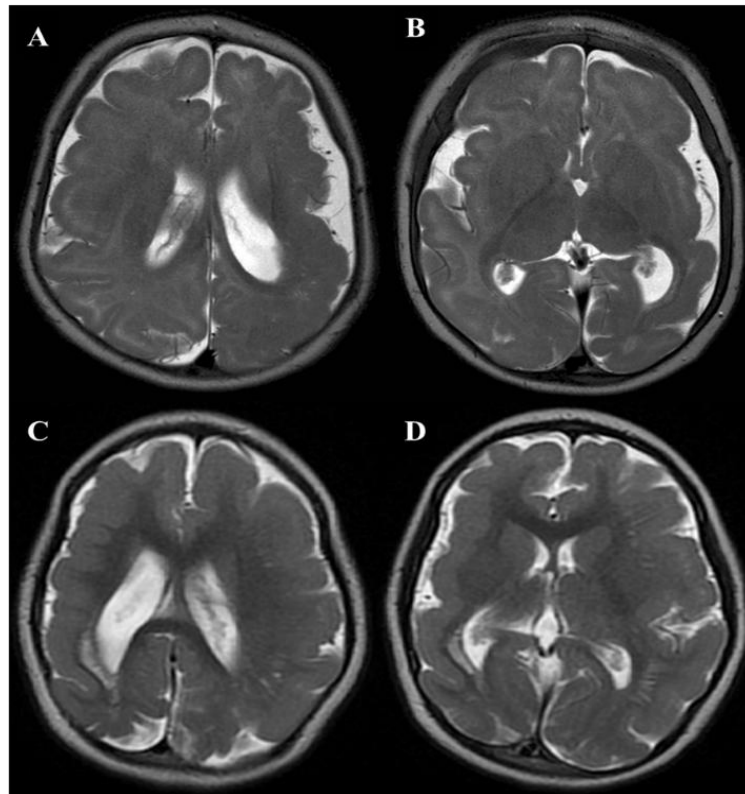


Fig. 4

MRI of Patient 2 (**A, B**) at the age of 5 months and Patient 3 (**C, D**) at the age of 4 years. The T2-weighted axial images demonstrate hemispherical asymmetry, diffuse pachygyria with a few broad gyri and shallow sulci, wide gray matter, and indistinct white-grey matter border in certain areas. The white matter is thin and the ventricles are asymmetrically enlarged,. The Virchow-Robin spaces are dilated.

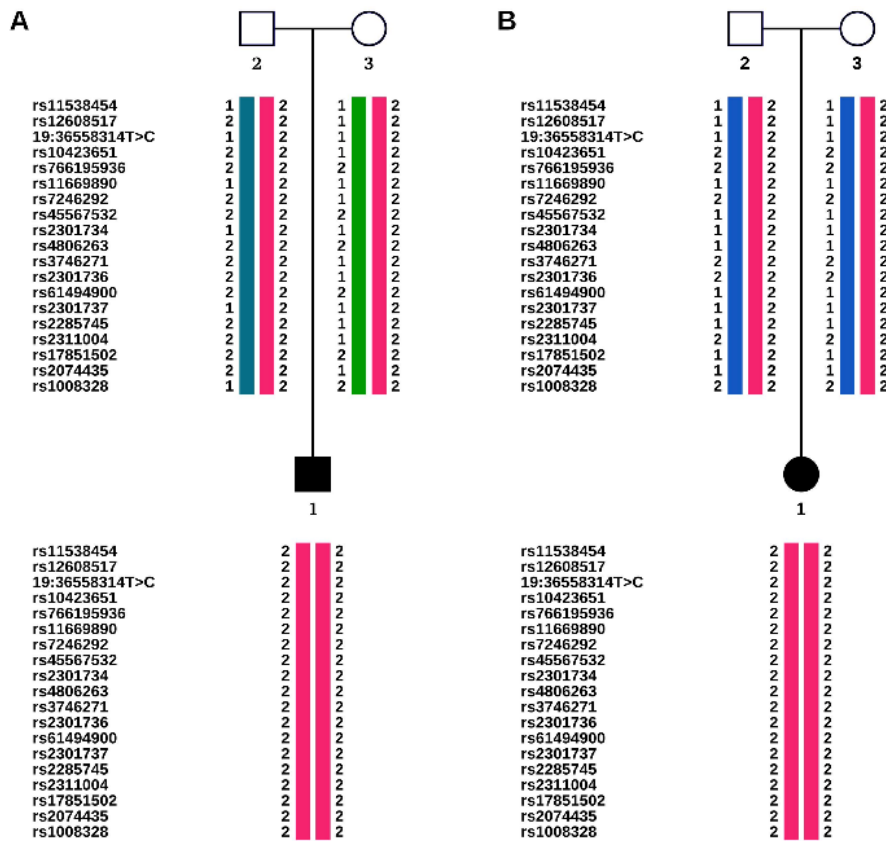


Fig. 5

Haplotype analysis of the families of Patient 2 (**A**) and 3 (**B**). Except the 19.36558314T>C unique variant, all the other examined SNPs are listed by their reference numbers. The identical haplotypes are coloured matched. The haplotype linked with the causative mutation is coloured magenta.

SNP: single-nucleotide polymorphism

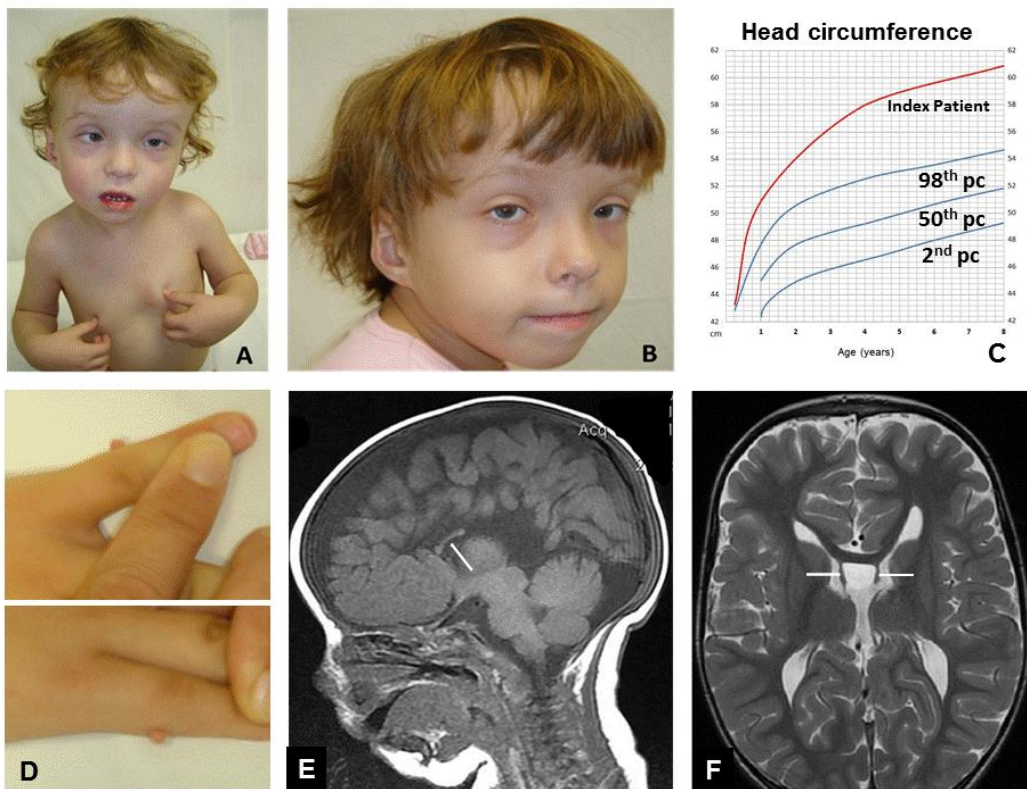


Fig. 6

Patient 4. Photographs, head circumference chart and brain MR images.

(A and B) The patient at the age of 2 (A) and 6 (B) years. Note prominent forehead, arched eyebrows, strabismus, flat, wide nasal bridge, short nose with a broad tip, long philtrum, small lower jaw and low-set ears with abnormally modelled helices.

(C) The chart shows the progressive growth of the head circumference.

(D) Bilateral skin tags on the fifth fingers.

(E) Sagittal T1-weighted MR image at the age of 3 months shows the partial agenesis of the corpus callosum with a thin remnant of the anterior part of the body (arrow).

(F) Axial T2-weighted MR image at the age of 4 years demonstrates the anterior part of the corpus callosum, dilated ventricles and widely separated leaves (arrows) of the septum pellucidum.

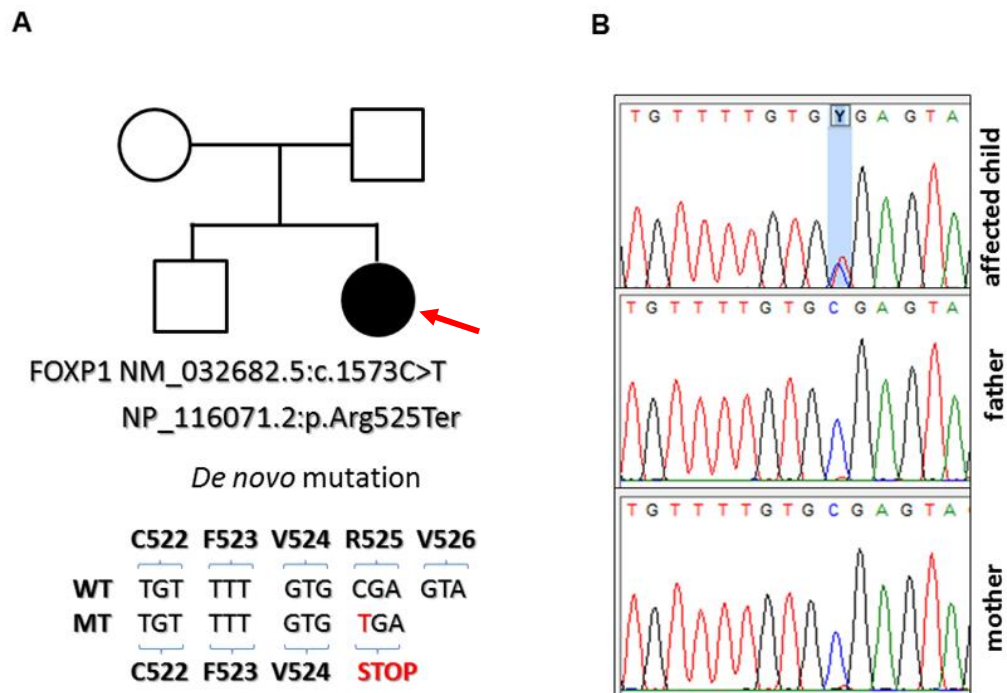


Fig. 7

Patient 4. *FOXP1* mutation.

(A) Mutation in *FOXP1* gene at c.1573 position results in a STOP codon. The mutation is very likely *de novo* since it was absent in the parents.

(B) The mutated position is highlighted in the DNA sequence of the affected child.

Y=T/C

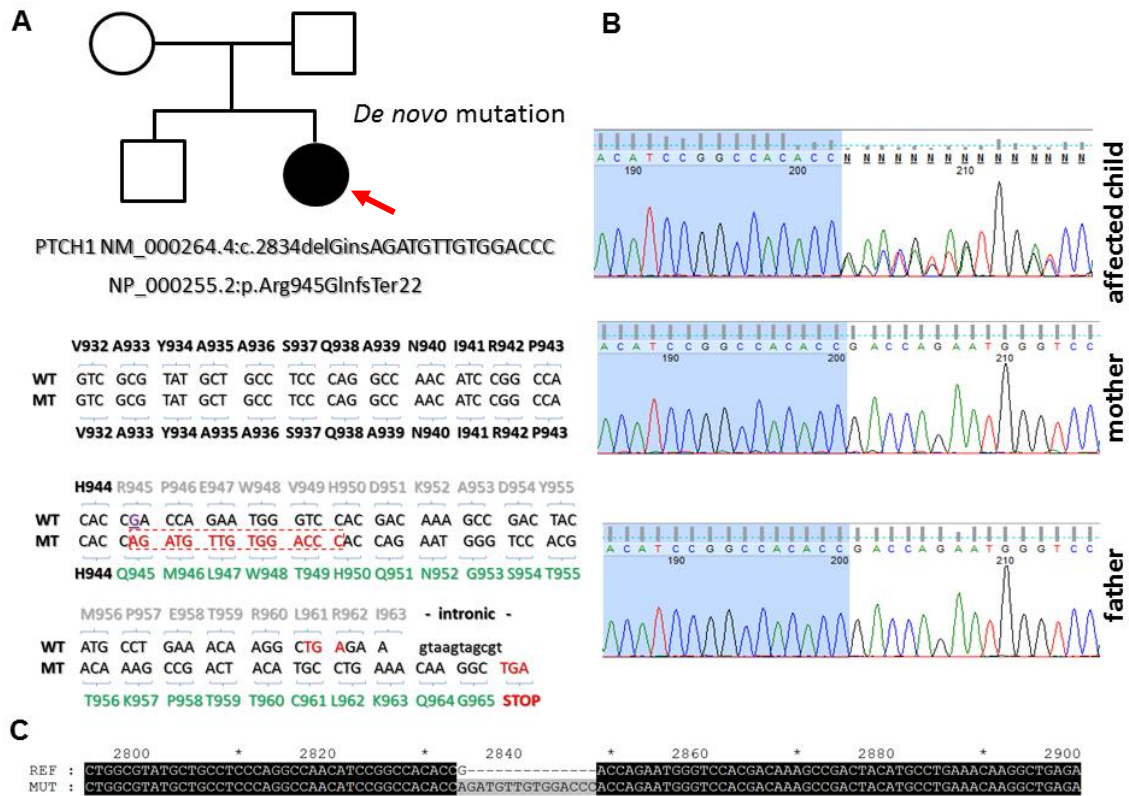


Fig. 8

Patient 4. *PTCH1* mutation.

(A) The complex *PTCH1* variant caused by a single-nucleotide deletion and a 15 bp long insertion in exon 17 which causes a premature STOP codon (p.Arg945GlnfsTer22). The mutated portion of the sequence is highlighted in red. The mutation is very likely *de novo* since it was absent in the parents.

(B) The presence of *PTCH1* mutation at DNA level confirmed by Sanger sequencing in the affected child. It is absent in the parents. The complex mutation starts after the highlighted portion of the sequence (blue).

(C) The sequence alignment of the reference and mutated *PTCH1* alleles.

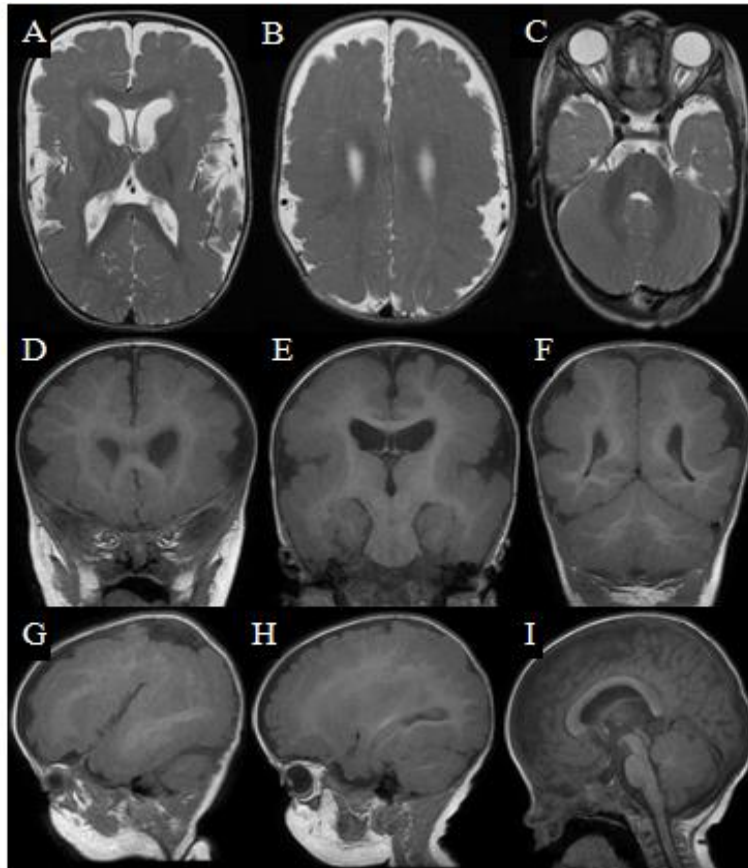


Fig. 9

Patient 5. MR images at the age of 7 months.

T2-weighted axial (A-C), T1-weighted coronal (D-F), T1-weighted parasagittal (G-H) and midsagittal (I) images reveal bilateral moderate dilatation of the lateral ventricles and wide Sylvian fissures. The extra-axial spaces are also slightly enlarged. Irregular small gyri with cortical thickening compatible with polymicrogyria can be seen bilaterally in the perisylvian, frontal, parietal and temporal areas with indistinct margin between the grey and white matter. The thick corpus callosum shows an abnormal shape. Wide cavum septi pellucidi and dilated Virchow-Robin spaces can also be observed.

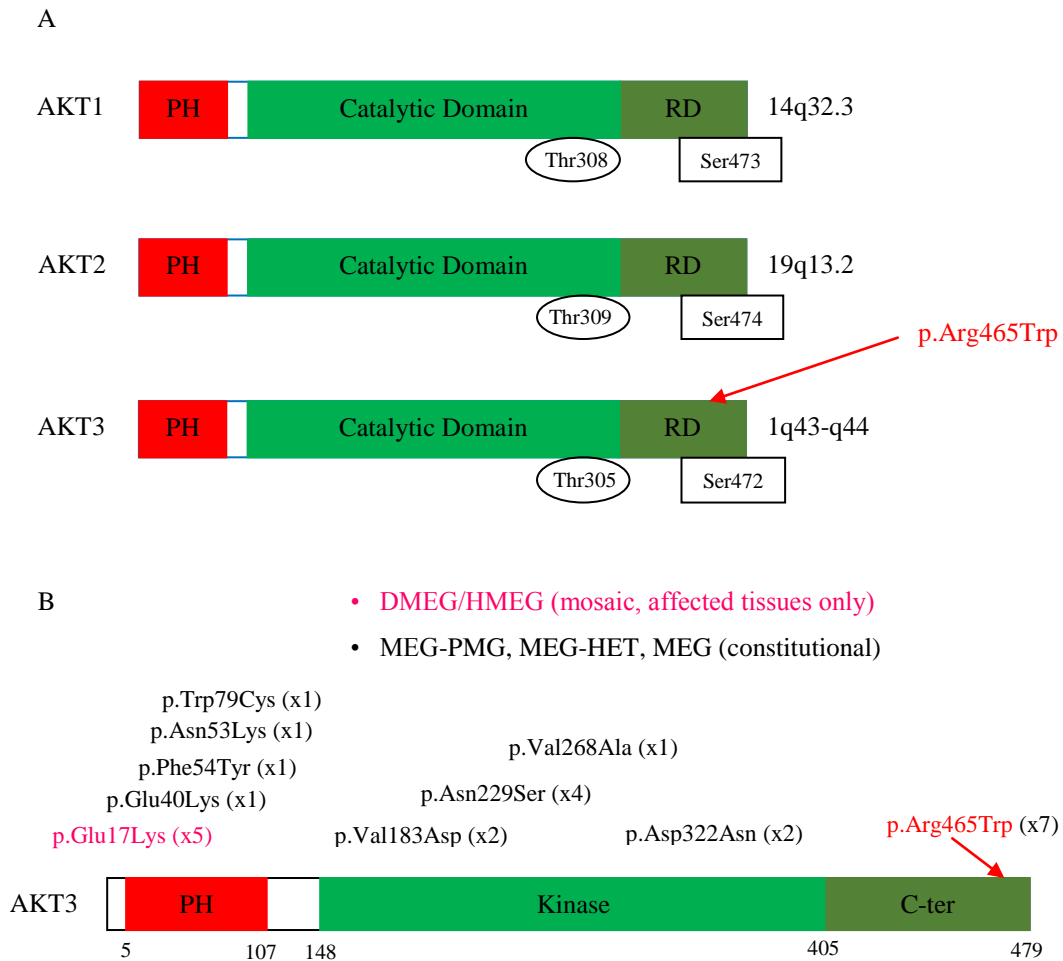


Fig. 10

(A) Domain structure of AKT isoforms. AKT3 contains 479 amino acids. Each of the AKT isoforms contains a pleckstrin homology (PH) domain in the N-terminal region followed by a linker region connecting the PH domain to the kinase (catalytic) domain and a regulatory C-terminal region (RD). The constitutional heterozygous missense variant of *AKT3* (c.1393C>T) in Patient 5 leads to a change of arginine into tryptophan at the position 465 in the regulatory C-terminal region (arrow) of the AKT3 protein, causing activation of the AKT-pathway. (*Figure and legend after Cohen, 2013*).

(B) Mutations identified in *AKT3* until April 2017 are shown, including Patient 5 in this study, along with the numbers of patients with these mutations in brackets.

DMEG: dysplastic megalencephaly, HET: heterotopia, HMEG: hemimegalencephaly, MEG: megalencephaly, PMG: polymicrogyria

(Alcantara D, Timms AE, Gripp K, Baker L, Park K, Collins S, et al. Mutations of *AKT3* are associated with a wide spectrum of developmental disorders including extreme megalencephaly. *Brain* 2017;**140**:2610-2622).

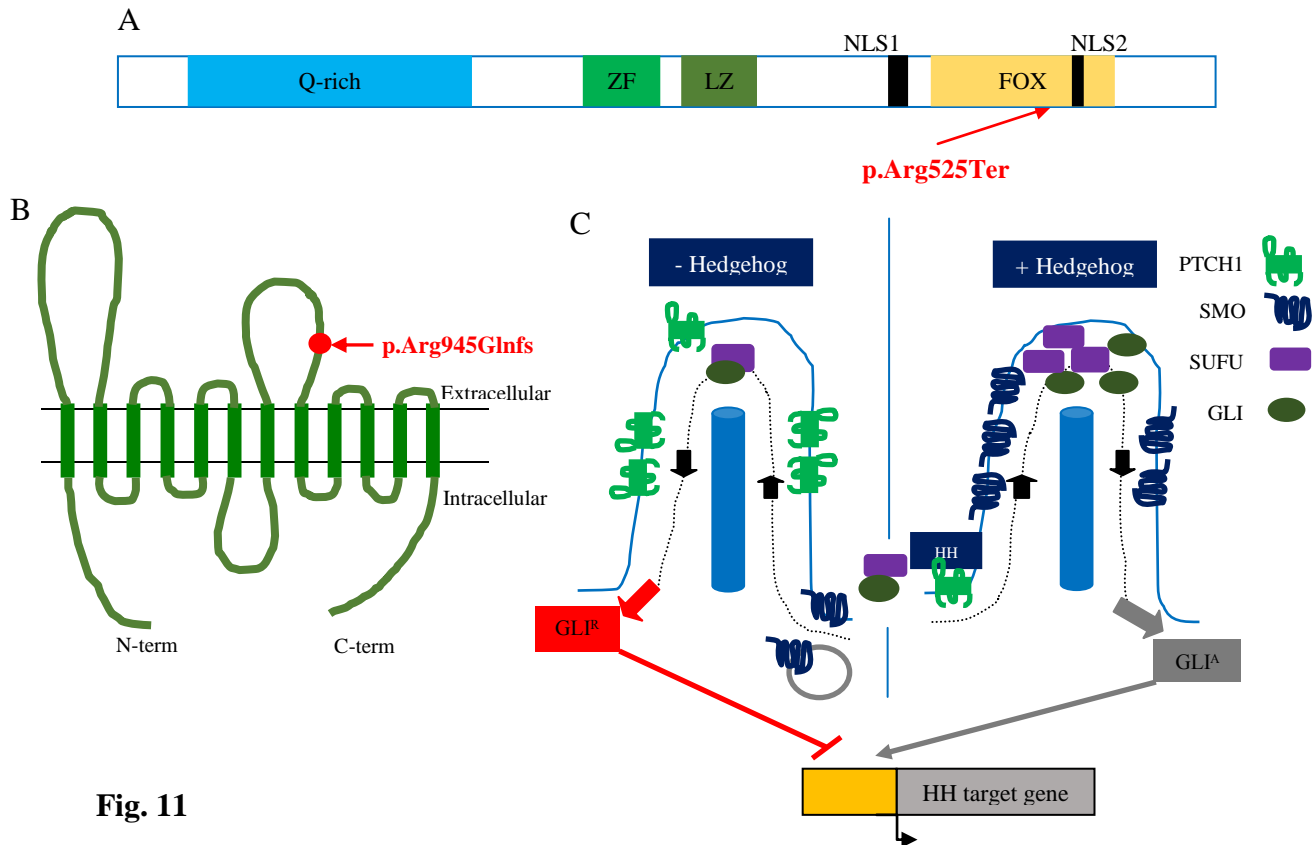


Fig. 11

FOXP1 protein. PTCH1 protein and SHH signalling.

(A) The FOXP1 protein is 677 amino acid long and its major domains are: a glutamine rich region (Q-rich), zinc finger (ZF) leucine zipper (LZ) and forkhead box (FOX) domains, and two nuclear localization signals (NLS1 and NLS2). The *de novo* heterozygous Arg525Ter change in Patient 1 is located in the FOX domain (arrow).

(B) The PTCH1 protein (Hedgehog receptor) consists of 1447 amino acids with 12 transmembrane regions, an intracellular and two extracellular loops. The *de novo* heterozygous Arg945GlnfsTer22 mutation in Patient 4 is located to one of the extracellular loops (arrow), presumably leading to protein truncation, or nonsense-mediated mRNA decay.

(C) Hedgehog (HH) signalling. In the absence of HH ligand, the HH receptor PTCH1 is enriched in cilia and the seven-transmembrane Smoothed (SMO) is excluded from cilia and maintained into an inactive conformation. The GLI (Glioblastoma (GLI) transcription factors (GLI2 and GLI3) enter cilia in complex with their partner and inhibitor SUFU (Suppressor of Fused) and become processed into transcriptional repressors (Gli^R) either inside cilia or after exit from the cilia. In the presence of HH ligand, PTCH1 disappears from the cilium and SMO accumulates in cilia in an active conformation. Active SMO prevents the processing of GLI into Gli^R and promotes the formation of the transcriptional activator form of GLI (Gli^A). (Figure and legend after Nachury, 2014)

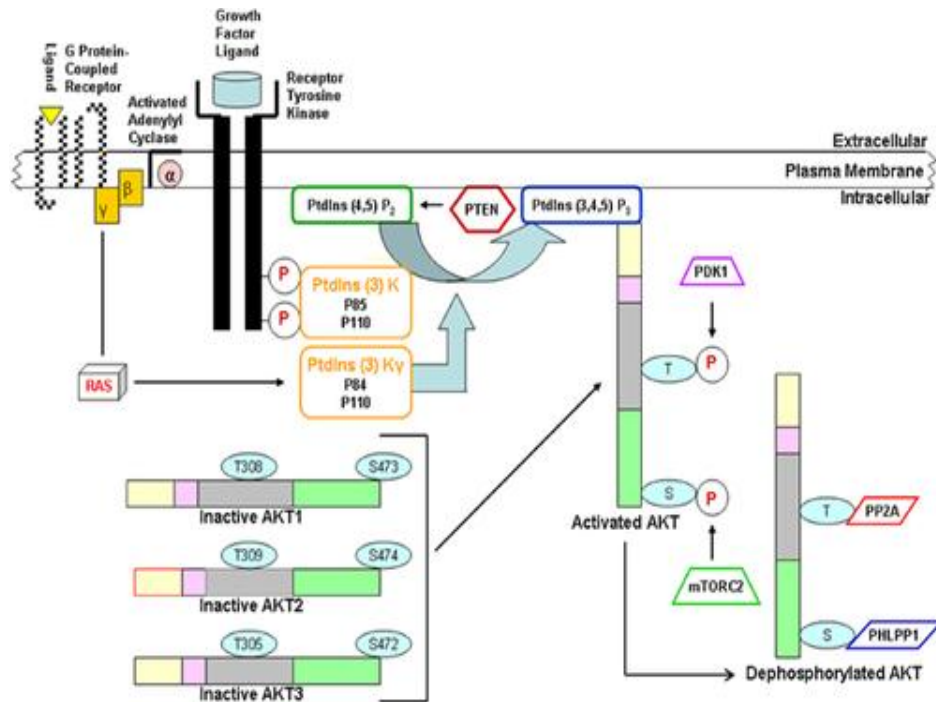


Fig. 12

Schematic illustration of the PI3K-AKT-mTOR pathway.

Class IA PI3K (Ptdins (3) K on the figure) is a heterodimer that consists of a p85 regulatory subunit and a p110 catalytic subunit. The regulatory subunit p85 binds to phospho-tyrosine residues on activated receptor tyrosine kinases. This binding both relieves the basal inhibition of p110 by p85 and recruits the p85-p110 heterodimer to its substrate phosphatidylinositol-4,5-bisphosphate [Ptdins (4,5) P₂, or PIP₂] at the plasma membrane leading to the synthesis of phosphatidylinositol-3,4,5-triphosphate [Ptdins (3,4,5) P₃, or PIP₃]. PTEN (phosphatase and tensin homologue) dephosphorylates PIP₃ and therefore terminates PI3K (Ptdins (3) K) signalling. The three isoforms of AKT are the most widely studied effectors of PI3K signalling. AKT undergoes membrane recruitment binding to Ptdins (3,4,5)P₃ (PIP₃) and the inactive forms of the AKT become activated by this attachment. This process of activation involves phosphorylation of threonine in the kinase domain of AKT by phosphoinositide-dependent protein kinase 1 (PDK1) and phosphorylation of serine in the regulatory domain of AKT by mammalian target of rapamycin complex 2 (mTORC2). Following such activation, the inactive AKT form is re-established through the action of protein phosphatases. The Thr residues are dephosphorylated by phosphatase 2A (PP2A), while the Ser residue of AKT3 is targeted

by the isoform 1 of the pleckstrin homology domain leucine-rich repeat protein phosphatases (PHLPP1 and PHLPP2). Downstream effects of AKT activation include cell growth, proliferation, survival, apoptosis, migration, metabolism and several other functions. (*Figure and legend after Cohen, 2013*)

REFERENCES

- Abecasis GR, Cherny SS, Cookson WO, Cardon LR. Merlin-rapid analysis of dense genetic maps using sparse gene flow trees. *Nat Genet* 2002;**30**:97-101.
- Alcantara D, Timms AE, Gripp K, Baker L, Park K, Collins S, et al. Mutations of *AKT3* are associated with a wide spectrum of developmental disorders including extreme megalencephaly. *Brain* 2017;**140**:2610-2622.
- Bacon C, Schneider M, Le Magueresse C, Froehlich H, Sticht C, Gluch C, et al. Brain-specific *Foxp1* deletion impairs neuronal development and causes autistic-like behaviour. *Mol Psychiatry* 2015;**20**:632-639.
- Ballif BC, Rosenfeld JA, Traylor R, Theisen A, Bader PI, Ladda RL, et al. High-resolution array CGH defines critical regions and candidate genes for microcephaly, abnormalities of the corpus callosum, and seizure phenotypes in patients with microdeletions of 1q43q44. *Hum Genet* 2012;**131**:145-156.
- Biever A, Valjent E, Puighermanal E. Ribosomal protein S6 phosphorylation in the nervous system: from regulation to function. *Front Mol Neurosci* 2015;**8**:75. doi:10.3389/fnmol.2015.00075. eCollection 2015.
- Bilgüvar K, Öztürk AK, Louvi A, Kwan KY, Choi M, Tatli B, et al. Whole-exome sequencing identifies recessive *WDR62* mutations in severe brain malformations. *Nature* 2010;**467**:207-211.
- Bogoyevitch MA, Yeap YYC, Zhengdong Q, Ngoel KR, Yip YY, Zhao TT, et al. WD40-repeat protein 62 is a JNK-phosphorylated spindle pole protein required for spindle maintenance and timely mitotic progression. *J Cell Sci* 2012;**125**:5096-5109.
- Bond J, Roberts E, Mochida GH, Hampshire DJ, Scott S, Askham JM et al. *ASPM* is a major determinant of cerebral cortical size. *Nat Gen* 2002;**32**:316-320.
- Bond J, Scott S, Hampshire DJ, Springell K, Corry P, Abramowicz MJ, et al. Protein-truncating mutations in *ASPM* cause variable reduction in brain size. *Am J Hum Genet* 2003;**73**:1170-1177.
- Briscoe J, Théron PP. The mechanisms of Hedgehog signalling and its roles in development and disease. *Nat Rev Mol Cell Biol* 2013;**14**:416-429.
- Capecchi MR, Pozner A. *ASPM* regulates symmetric stem cell division by tuning Cyclin E ubiquitination. *Nat Commun* 2015;**19**:6:8763. doi:10.1038/ncomms9763.
- Carmena M, Wheelock M, Funabiki H, Earnshaw WC. The chromosomal passenger

- complex (CPC): from easy rider to the godfather of mitosis. *Nat Rev Mol Cell Biol* 2012;**13**:789-803.
- Carpenter D, Stone DM, Brush J, Ryan A, Armanini M, Frantz G, et al. Characterization of two patched receptors for the vertebrate hedgehog protein family. *Proc Natl Acad Sci USA* 1998;**95**:13630-13634.
- Chang CC, Chow CC, Tellier LC, Vattikuti S, Purcell SM, Lee JJ. Second-generation PLINK: rising to the challenge of larger and richer datasets. *Gigascience* 2015;<https://doi.org/10.1186/s13742-015-0047-8>.
- Chen JF, Zhang Y, Wilde J, Hansen K, Lai F, Niswander L. Microcephaly disease gene Wdr62 regulates mitotic progression of embryonic neural stem cells and brain size. *Nat Commun* 2014;**30**;5:3885. doi:10.1038/ncomms4885.
- Cheung M, Testa JR. Diverse mechanisms of AKT pathway activation in human malignancy. *Curr Cancer Drug Targets* 2013;**13**:234-244.
- Chung BK, Eydoux P, van Karnebeek CD, Gibson WT. Duplication of *AKT3* is associated with macrocephaly and speech delay. *Am J Med Genet Part A* 2014;**164A**:1868-1869.
- Cohen MM. The AKT genes and their roles in various disorders. *Am J Med Genet Part A* 2013;**161A**:2931-2937.
- Conti V, Pantaleo M, Barba C, Baroni G, Mei D, Buccoliero AM, et al. Focal dysplasia of the cerebral cortex and infantile spasms associated with somatic 1q21.1-q44 duplication including the *AKT3* gene. *Clin Genet* 2015;**88**:241-247.
- Dehay C, Kennedy H. Cell-cycle control and cortical development. *Nat Rev Neurosci* 2007;**8**:438-450.
- Depienne C, Nava C, Keren B, Heide S, Rastetter A, Passemard S, et al. Genetic and phenotypic dissection of 1q43q44 microdeletion syndrome and neurodevelopmental phenotypes associated with mutations in *ZBTB18* and *HNRNPU*. *Hum Genet* 2017;**136**:463-479.
- D’Gama AM, Woodworth MB, Hossain AA, Bizzotto S, Hatem NE, LaCoursiere CM, et al. Somatic mutations activating the mTOR pathway in dorsal telencephalic progenitors cause continuum of cortical dysplasias. *Cell Rep* 2017;**21**:3754-3766.
- Easton RM, Cho H, Roovers K, Shineman DW, Mizrahi M, Forman MS, et al. Role for Akt3/protein kinase B γ in attainment of normal brain size. *Mol Cell Biol* 2005;**25**:1869-1878.
- Engelman JA, Luo J, Cantley LC. The evolution of phosphatidylinositol 3-kinases as

- regulators of growth and metabolism. *Nature Rev Genet* 2006;**7**:606-619.
- Estruch SB, Graham SA, Quevedo M, Vino A, Dekkers DHW, Deriziotis P, et al. Proteomic analysis of FOXP proteins reveals interactions between cortical transcription factors associated with neurodevelopmental disorders. *Hum Mol Genet* 2018;**27**:1212-1227.
- Farag HG, Froehler S, Oexle K, Ravindran E, Schindler D, Staab T, et al. Abnormal centrosome and spindle morphology in a patient with autosomal recessive primary microcephaly type 2 due to compound heterozygous WDR62 gene mutation. *Orphanet J Rare Dis* 2013;**8**:178. doi:10.1186/1750-1172-8-178.
- Ferland RJ, Cherry TJ, Preware PO, Morrissey EE, Walsh CA. Characterization of Foxp2 and Foxp1 mRNA and protein in the developing and mature brain. *J Comp Neurol* 2003;**460**:266-279.
- Fish JL, Kosodo Y, Enard W, Pääbo S, Huttner WB. Aspm specifically maintains symmetric proliferative divisions of neuroepithelial cells. *Proc Natl Acad Sci USA* 2006;**103**:10438-10443.
- Fish JL, Dehay C, Kennedy H, Huttner WB. Making bigger brains – the evolution of neural-progenitor-cell division. *J Cell Sci* 2008;**121**:2783-2793.
- Fujii K, Miyashita T. Gorlin syndrome (nevroid basal cell carcinoma syndrome): Update and literature review. *Pediatr Int* 2014;**56**:667-674.
- Gai D, Haan E, Scholar M, Nicholl J, Yu S. Phenotypes of *AKT3* deletion: a case report and literature review. *Am J Med Genet Part A* 2015;**167A**:174-179.
- Gai M, Bianchi FT, Vagnoni C, Verni F, Bonaccorsi S, Pasquero S, et al. ASPM and CITK regulate spindle orientation by affecting the dynamics of astral microtubules. *EMBO Rep* 2016;**17**:1396-1409.
- Gianferante DM, Rotunno M, Dean M, Zhou W, Hicks BD, Wyatt K, et al. Whole-exome sequencing of nevroid basal cell carcinoma syndrome families and review of Human Gene Mutation Database *PTCH1* mutation data. *Mol Genet Genomic Med* 2018;**6**:1168-1180.
- Golson ML, Kaestner KH. Fox transcription factors: from development to disease. *Development* 2016;**143**:4558-4570.
- Gong X, Qian H, Cao P, Zhao X, Zhou Q, Lei J, et al. Structural basis for the recognition of Sonic Hedgehog by human Patched1. *Science* 2018;**361**(6402). pii: eaas8935. doi: 10.1126/science.aas8935.
- Goodrich LV, Milenković L, Higgins KM, Scott MP. Altered neural cell fates and

- medulloblastoma in mouse *patched* mutants. *Science* 1997;**277**:1109- 1113.
- Gorlin RJ. Nevoid basal cell carcinoma (Gorlin) syndrome. *Genet Med* 2004;**6**:530-539.
- Hahn H, Wicking C, Zaphiropoulos PG, Gailani MR, Shanley S, Chidambaram A, et al. Mutations of the human homolog of *Drosophila patched* in the nevoid basal cell carcinoma syndrome. *Cell* 1996;**85**:841-851.
- Hamdan FF, Daoud H, Rochefort D, Piton A, Gauthier J, Langlois M, et al. De novo mutations in *FOXP1* in cases with intellectual disability, autism, and language impairment. *Am J Hum Genet* 2010;**87**:671-678.
- Harada A, Miya F, Utsunomiya H, Kato M, Yamanaka T, Tsunoda T, et al. Sudden death in a case of megalencephaly capillary malformation associated with a de novo mutation in *AKT3*. *Childs Nerv Syst* 2015;**31**:465-471.
- Hemming IA, Forrest ARR, Shipman P, Woodward KJ, Walsh P, Ravine DG, et al. Reinforcing the association between distal 1q CNVs and structural brain disorder: a case of a complex 1q43-q44 CNV and a review of the literature. *Am J Med Genet Part B* 2016;**171B**:458-467.
- Hiatt JB, Pritchard CC, Salipante SJ, O’Roak BJ, Shendure J. Single molecule molecular inversion probes for targeted, high-accuracy detection of low-frequency variation. *Genome Res* 2013;**23**:843-854.
- Higgins J, Midgley C, Bergh AM Bell SM, Askham JM, Roberts E et al. Human ASPM participates in spindle organisation, spindle orientation and cytokinesis. *BMC Cell Biol* 2010;**11**:85. doi 10.1186/1471-2121-11-85.
- Hussain K, Challis B, Rocha N, Payne F, Minic M, Thompson A, et al. An activating mutation of *AKT2* and human hypoglycaemia. *Science* 2011;**334**:474.
- Jamuar SS, Lam ATN, Kircher M, D’Gama AM, Wang J, Barry BJ, et al. Somatic mutations in cerebral cortical malformations. *N Engl J Med* 2014;**371**:733-743.
- Jansen LA, Mirzaa GM, Ishak GE, O’Roak BJ, Hiatt JB, Roden WH, et al. PI3K/AKT pathway mutations cause a spectrum of brain malformations from megalencephaly to focal cortical dysplasia. *Brain* 2015;**138**:1613-1528.
- Jayaraman D, Bae BI, Walsh C. The genetics of primary microcephaly. *Ann Rev Genom Hum Genet* 2018;**19**:177-200.
- Jayaraman D, Kodani A, Gonzales DM, Mancias JD, Mochoda GH, Vagnoni C, et al.

- Microcephaly proteins Wdr62 and Aspm define a mother centriole complex regulating centriole biogenesis, apical complex, and cell fate. *Neuron* 2016;**92**:813-828.
- Jia Y, Wang Y, Xie J. The Hedgehog pathway: role in cell differentiation, polarity and proliferation. *Arch Toxicol* 2015;**89**:179-191.
- Johnson MB, Sun X, Kodani A, Borges-Monroy R, Girsakis KM, Ryu SC, et al. Aspm knockout ferret reveals an evolutionary mechanism governing cerebral cortical size. *Nature* 2018;**556**:370-375.
- Kimonis VE, Goldstein AM, Pastakia B, Yang ML, Kase R, DiGiovanna JJ, et al. Clinical manifestations in 105 persons with nevoid basal cell carcinoma syndrome. *Am J Med Genet* 1997;**69**:299-308.
- Kimonis VE, Mehta SG, DiGiovanna JJ, Bale SJ, Pastakia B. Radiological features in 82 patients with nevoid basal cell carcinoma (NBCC or Gorlin) syndrome. *Genet Med* 2004;**6**:495-502.
- Kimonis VE, Singh KE, Zhong R, Pastakia B, DiGiovanna JJ, Bale SJ. Clinical and radiological features in young individuals with nevoid basal cell carcinoma syndrome. *Genet Med* 2013;**15**:79-83.
- Kobayashi E, Bagshaw AP, Jansen A, Andermann F, Andermann E, Gotman J, et al. Intrinsic epileptogenicity in polymicrogyric cortex suggested by EEG-fMRI BOLD responses. *Neurology* 2005;**64**:1263-1266.
- Kouprina N, Pavlicek A, Collins NK, Nakano M, Noskov VN, Ohzeki JJ, et al. The microcephaly ASPM gene is expressed in proliferating tissues and encodes for a mitotic spindle protein. *Hum Mol Genet* 2005;**14**:2155-2165.
- Lee JH, Huynh M, Silhavy JL, Kim S, Dixon-Salazar T, Heiberg A, et al. *De novo* somatic mutations in components of the PI3K-AKT3-mTOR pathway cause hemimegalencephaly. *Nat Genet* 2012;**44**:941-945.
- Le Fevre AK, Taylor S, Malek NH, Horn D, Carr CW, Abdul-Rahman OA, et al. *FOXP1* mutations cause intellectual disability and a recognizable phenotype. *Am J Med Genet Part A* 2013;**161A**:3166-3175.
- Létard P, Drunat S, Vial Y, Duerinckx S, Ernault A, Amram D, Arpin S, Bertoli M, et al. Autosomal recessive primary microcephaly due to ASPM mutations: An update. *Hum Mutat* 2018;**39**:319-332.
- Li D, Roberts R. WD-repeat proteins: structure characteristics, biological function, and their

- involvement in human diseases. *Cell Mol Life Sci* 2001;**58**:2085-2097.
- Li S, Weidenfeld J, Morrisey EE. Transcriptional and DNA binding activity of the Foxp1/2/4 family is modulated by heterotypic and homotypic protein interactions. *Mol Cell Biol* 2004;**24**:809-822.
- Li X, Xiao J, Fröhlich H, Tu X, Li L, Xu Y, et al. Foxp1 regulates cortical radial migration and neuronal morphogenesis in developing cerebral cortex. *PloS One* 2015;doi: 10.1371/journal.pone.0127671.
- Lindhurst MJ, Sapp JC, Teer JK, Johnston JJ, Finn EM, Peters K, et al. A mosaic activating mutation in *AKT1* associated with the Proteus syndrome. *N Engl J Med* 2011;**365**:611-619.
- Lindström E, Shimokawa T, Toftgård R, Zaphiropoulos PG. PTCH mutations: Distribution and analysis. *Hum Mutat* 2006;**27**:215-219.
- Manning BD, Toker A. AKT/PKB signalling: Navigating the network. *Cell* 2017;**169**:381-405.
- Marigo V, Davey RA, Zuo Y, Cunningham JM, Tabin CJ. Biochemical evidence that Patched is the Hedgehog receptor. *Nature* 1996;**384**:176-179.
- Mazzuocolo LD, Martínez MF, Muchnik C, Azurmendi PJ, Stengel F. Síndrome de carcinoma basocelular nevoide con agenesia de cuerpo calloso, mutación en PTCH1 y ausencia de carcinoma basocelular. *Medicina (Buenos Aires)* 2014;**74**:307-310.
- Meerschaut I, Rochefort D, Revençu N, Pètre J, Corssello C, Rouleau GA, et al. *FOXP1*-related intellectual disability syndrome: a recognisable entity. *J Med Genet* 2017;**54**:613-623.
- Mirzaa GM, Campbell CD, Solovieff N, Goold CP, Jansen LA, Menon S, et al. Association of *MTOR* mutations with developmental brain disorders, including megalencephaly, focal cortical dysplasia, and pigmentary mosaicism. *JAMA Neurol* 2016;**73**:836-845.
- Mirzaa GM, Poduri A. Megalencephaly and hemimegalencephaly: breakthroughs in molecular etiology. *Am J Med Genet Part C* 2014;**166C**:156-172.
- Mirzaa GM, Rivière, Dobyns WB. Megalencephaly syndromes and activating mutations in the PI3K-AKT pathway: MPPH and MCAP. *Am J Med Genet Part C Semin Med Genet* 2013;**163C**:122-130.
- Morita K, Naruto T, Tanimoto K, Yasukawa C, Oikawa Y, Masuda K, et al.

- Simultaneous detection of both single nucleotide variations and copy number alterations by next-generation sequencing in Gorlin syndrome. *PloS One* 2015;doi: 10.1371/journal.pone.0140480.
- Mundi PS, Sachdev J, McCourt C, Kalinsky K. AKT in cancer: new molecular insights and advances in drug development. *Br J Clin Pharmacol* 2016;**82**:943-956.
- Nakamura K, Kato M, Tohyama J, Shiohama T, Hayasaka K, Nishiyama K, et al. *AKT3* and *PIK3R2* mutations in two patients with megalencephaly-related syndromes: MCAP and MPPH. *Clin Genet* 2014;**85**:396-398.
- Negishi Y, Miya F, Hattori A, Johmura Y, Nakagawa M, Ando N, et al. A combination of genetic and biochemical analyses for the diagnosis of PI3K-AKT-mTOR pathway-associated megalencephaly. *BMC Med Genet* 2017;18:4. doi: 10.1186/s12881-016-0363-6.
- Nellist M, Schot R, Hoogeveen-Westerveld M, Neuteboom RF, van der Louw EJTM, Lequin MH, et al. Germline activating *AKT3* mutation associated with megalencephaly, polymicrogyria, epilepsy and hypoglycaemia. *Mol Genet Metab* 2015;**114**:467-473.
- Nicholas AK, Khushid M, Désir J, Carvalho OP, Cox JJ, Thornton G, et al. WDR62 is associated with the spindle pole and is mutated in human microcephaly. *Nat Genet* 2010;**42**:1010-1014
- Nigg EA, Holland AJ. Once and only once: mechanisms of centriole duplication and their deregulation in disease. *Nat Rev Mol Cell Biol* 2018;**19**:297-312.
- Passemard S, Titomanlio L, Elmaleh M, Afenjar A, Alessandri JL, Andria G, et al. Expanding the clinical and neuroradiologic phenotype of primary microcephaly due to *ASPM* mutations. *Neurology* 2009;**73**:962-969.
- Pavone P, Praticò AD, Rizzo R, Corsello G, Ruggieri M, Parano E et al. A clinical review in megalencephaly. A large brain as a possible sign of cerebral impairment. *Medicine (Baltimore)* 2017;**96(26)**:e6814. doi: 10.1097/MD.00000000000006814.
- Pellegrini C, Maturo MG, Di Nardo L, Ciciarelli V, Garcia-Rodrigo CG, Fargnoli MC. Understanding the molecular genetics of basal cell carcinoma. *Int J Mol Sci* 2017;18. pii: E2485. doi: 10.3390/ijms18112485.
- Pfeifer GP. Mutagenesis at methylated CpG sequences. *Curr Top Microbiol Immunol* 2006;**301**:259-281.
- Phillips M, Pozzo-Miller L. Dendritic spine dysgenesis in autism related disorders.

- Neurosci Lett* 2015;**601**:30-40.
- Poduri A, Evrony GD, Cai X, Elhosary PC, Beroukhir R, Lehtinen MK, et al. Somatic activation of *AKT3* causes hemispheric developmental brain malformations. *Neuron* 2012;**74**:41-48.
- Prosser SL, Pelletier L. Mitotic spindle assembly in animal cells: a fine balancing act. *Nat Rev Mol Cell Biol* 2017;**18**:187-201.
- Qin X, Jiang B, Zhang Y. 4E-BP1, a multifactor regulated multifunctional protein. *Cell Cycle* 2016;**15**:781-786.
- Rivière JB, Mirzaa GM, O’Roak BJ, Beddaoui M, Alcantara D, Conway RL, et al. *De novo* germline and postzygotic mutations in *AKT3*, *PIK3R2* and *PIK3CA* cause a spectrum of related megalencephaly syndromes. *Nat Genet* 2012;**44**:934-940.
- Rohatgi R, Milenkovic L, Scott MP. Patched1 regulates Hedgehog signaling at the primaty cilium. *Science* 2007;**317**:372- 376.
- Sgourdou P, Mishra-Gorur K, Saotome I, Henagariu O, Tuysuz B, Campos C, et al. Disruptions in asymmetric centrosome inheritance and WDR62-Aurora kinase B interactions in primary microcephaly. *Sci Rep* 2017;**7**:43708. doi:10.1038/srep43708.
- Shiohama T, Fujii K, Miyashita T, Mizuochi H, Uchikawa H, Shimojo N. Brain morphology in children with nevoid basal cell carcinoma syndrome. *Am J Med Genet* 2017;**173**:946-952.
- Shohayeb B, Lim NR, Ho U, Xu Z, Dottori M, Quinn L, et al. The role of WD40-repeat protein 62 (MCPH2) in brain growth: diverse molecular and cellular mechanisms required for cortical development. *Mol Neurobiol* 2018;**55**:5409-5424.
- Sollis E, Graham SA, Vino A, Froehlich H, Vreeburg M, Dimitropoulou D, et al. Identification and functional characterization of *de novo* *FOXP1* variants provides novel insights into the etiology of neurodevelopmental disorder. *Hum Mol Genet* 2016;**25**:546-557.
- Stahl JM, Sharma A, Cheung M, Zimmerman M, Cheng JQ, Bosenberg MW, et al. Deregulated Akt3 activity promotes development of malignant melanoma. *Cancer Res* 2004;**64**:7002-7010.
- Stirnemann CU, Petsalaki E, Russel RB, Müller CW. WD40 proteins propel cellular networks. *Trends Biochem Sci* 2010;**35**:565-574.
- Takagi M, Dobashi K, Nagahara K, Kato M, Nishimura G, Fukuzawa R, et al. A novel

- de novo* germline mutation Glu40Lys in *AKT3* causes megalencephaly with growth hormone deficiency. *Am J Med Genet Part A* 2017;**173A**:1071-1076.
- Takanashi J, Fujii K, Takano H, Sugita K, Kohno Y. Empty sella syndrome in nevoid basal cell carcinoma syndrome. *Brain Dev* 2000;**22**:272-274.
- Tan IL, Wojcinski A, Rallapalli H, Lao Z, Sanghrajka RM, Stephen D, et al. Lateral cerebellum is preferentially sensitive to high sonic hedgehog signaling and medulloblastoma formation. *Proc Natl Acad Sci USA* 2018;**115**:3392-3397.
- Teramitsu I, Kudo LC, London SE, Geschwind DH, White SA. Parallel *FoxP1* and *FoxP2* expression in songbird and human brain predicts functional interaction. *J Neurosci* 2004;**24**:3152-3163.
- Thiele H, Nürnberg P. HaploPainter: a tool for drawing pedigrees with complex haplotypes. *Bioinformatics* 2005;**21**:1730-1732.
- Tokuda S, Mahaffey CL, Monks B, Faulkner CR, Birnbaum MJ, Danzer ST, et al. A novel *Akt3* mutation associated with enhanced kinase activity and seizure susceptibility in mice. *Hum Mol Genet* 2011;**20**:988-999.
- Tschopp O, Yang ZZ, Brodbeck D, Dummler BA, Hemmings-Mieszczak M, Watanabe T, et al. Essential role of protein kinase B γ (PKB γ /Akt3) in postnatal brain development but not in glucose homeostasis. *Development* 2005;**132**:2943-2954.
- Uzquiano A, Gladwyn-Ng I, Nguyen L, Reiner O, Götz M, Matsuzaki F. et al. Cortical progenitor biology: key features mediating proliferation versus differentiation. *J Neurochem* 2018;doi:10.1111/jnc.14338.
- Veenstra-Knol HE, Scheewe JH, van der Vlist GJ, van Doorn ME, Ausems MGEM. Early recognition of basal cell naevus syndrome. *Eur J Pediatr* 2005;**164**:126-130.
- von der Hagen M, Pivarcsi M, Liebe J, von Bernuth H, Didonato N, Hennermann JB et al. *Dev Med Child Neurol* 2014;**56**:732-741.
- Wang B, Lin D, Li C, Tucker P. Multiple domains define the expression and regulatory properties of Foxp1 forkhead transcriptional repressors. *J Biol Chem* 2003;**278**:24259-24268.
- Wang D, Zeesman S, Tarnopolsky MA, Nowaczyk MJM. Duplication of *AKT3* as a cause of macrocephaly in duplication 1q43q44. *Am J Med Genet Part A* 2013;**161A**:2016-2019.
- Wang X, Tsai JW, Imai JH, Lian WN, Vallee RB, Shi SH. Asymmetric centrosome

inheritance maintains neural progenitors in the neocortex. *Nature* 2009;**461**:947-955.

Woods CG, Bond J, Enard W. Autosomal recessive primary microcephaly (MCPH): A review of clinical, molecular, and evolutionary findings. *Am J Hum Genet* 2005;**76**:717-728.

Yang ZJ, Ellis T, Markant SL, Read TA, Kessler JD, Bourboulas M, et al. Medulloblastoma can be initiated by deletion of *Patched* in lineage-restricted progenitors or stem cells. *Cancer Cell* 2008;**14**:135-145.

Yu TW, Mochida GH, Tischfield DJ, Sgaier SK, Flores-Sarnat L, Sergi CM. et al. Mutations in *WDR62*, encoding a centrosome-associated protein, cause microcephaly with simplified gyri and abnormal cortical architecture. *Nat Genet* 2010;**42**:1015-1020.

Zaqout S, Morris-Rosendahl D, Kaindl AM. Autosomal recessive primary microcephaly (MCPH): An update. *Neuropediatrics* 2017;**48**:135-14.